AD NUMBER

ADB007253

LIMITATION CHANGES

TO:

Approved for public release; distribution is unlimited.

FROM:

Distribution authorized to U.S. Gov't. agencies only; Test and Evaluation; APR 1975. Other requests shall be referred to Air Force Materials Lab., Wright-Patterson AFB, OH 45433.

AUTHORITY

AFML ltr 20 Oct 1978

AFML-TR-75-38

PART I

(12)

INVESTIGATION OF CAGE AND BEARING INSTABILITY IN DESPUN ANTENNA BEARINGS DUE TO CHANGES IN LUBRICATION PROPERTIES

BATTELLE'S COLUMBUS LABORATORIES

APRIL 1975

TECHNICAL REPORT AFML-TR-75-39, PART I

AIR FORCE WRIGHT AERONAUTICAL LABORATORY
AIR FORCE MATERIALS LABORATORY
Air Force Systems Command
Wright-Patterson Air Force Base, Ohio

Notice

When Government drawings, specifications, or other data are used for any purpose other than in connection with a definitely related Government procurement operation, the United States Government thereby incurs no responsibility nor any obligation whatsoever; and the fact that the government may have formulated, furnished, or in any way supplied the said drawings, specifications, or other data, is not to be regarded by implication or otherwise as in any manner licensing the holder or any other person or corporation, or conveying any rights or permission to manufacture, use, or sell any patented invention that may in any way be related thereto.

This technical report has been reviewed and is approved.

Mario P. Rivera

MARIO P. RIVERA
Project Monitor

FOR THE COMMANDER

Larry L. Fehrenbacher

LARRY L. FEHRENBACHER, Major, USAF
Chief, Lubricants and Tribology Branch
Nonmetallic Materials Division

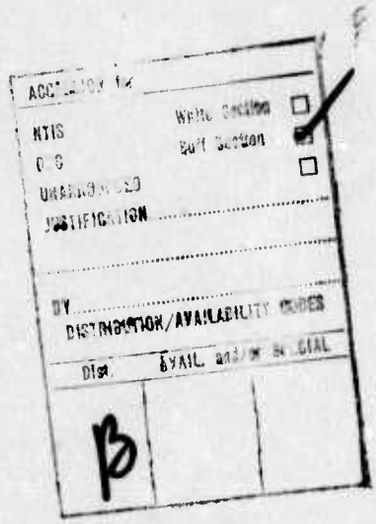

Copies of this report should not be returned unless return is required by security considerations, contractual obligations, or notice on a specific document.

AIR FORCE - 26-9-75 - 250

SECURITY CLASSIFICATION OF THIS PAGE *(When Data Entered)*

REPORT DOCUMENTATION PAGE

READ INSTRUCTIONS BEFORE COMPLETING FORM

1. REPORT NUMBER: AFML-TR-75-38 (Part I)
2. GOVT ACCESSION NO.: ---
3. RECIPIENT'S CATALOG NUMBER: ---

4. TITLE *(and Subtitle)*: Investigation of Cage and Bearing Instability in Despun Antenna Bearings Due to Changes in Lubricant Properties

5. TYPE OF REPORT & PERIOD COVERED: Summary, Jan. 31, 1974-Jan. 31, 1975
6. PERFORMING ORG. REPORT NUMBER: ---

7. AUTHOR(s): J. W. Kannel, S. S. Bupara, C. J. Pentlicki (COMSAT Laboratories)
8. CONTRACT OR GRANT NUMBER(s): F33615-74-C-5012

9. PERFORMING ORGANIZATION NAME AND ADDRESS: Battelle's Columbus Laboratories, 505 King Avenue, Columbus, Ohio 43201
10. PROGRAM ELEMENT, PROJECT, TASK AREA & WORK UNIT NUMBERS: 62102F, 7343 03 16

11. CONTROLLING OFFICE NAME AND ADDRESS: United States Air Force, Air Force Systems Command - HQ 4950th Test Wing, Wright-Patterson Air Force Base, Ohio 45433
12. REPORT DATE: April, 1975
13. NUMBER OF PAGES: 61

14. MONITORING AGENCY NAME & ADDRESS *(if different from Controlling Office)*: Summary rept. no. 1, 1 Feb 74 - 31 Jan 75
15. SECURITY CLASS. *(of this report)*: Unclassified
15a. DECLASSIFICATION/DOWNGRADING SCHEDULE

16. DISTRIBUTION STATEMENT *(of this Report)*: Distribution Limited to U.S. Government Agencies only.

17. DISTRIBUTION STATEMENT *(of the abstract entered in Block 20, if different from Report)*

18. SUPPLEMENTARY NOTES

19. KEY WORDS *(Continue on reverse side if necessary and identify by block number)*

Bearing Dynamics
Bearing Design
Bearing EHD
Cage Design
Cage Dynamics

20. ABSTRACT *(Continue on reverse side if necessary and identify by block number)*

A computer program is being developed for the purpose of investigating cage and bearing instability in a despun antenna bearings. The program utilizes empirical inputs to ensure accuracy of the analytical modeling and comparison with experimental cage-dynamics data are being made to validate the computer predictions. As a result of the experimental and analytical studies conducted thus far, a stability criterion is being postulated. One form of this criterion, denoting the state of stability of the system, can be written as $D_p = 4C_{mn}^2/M_e C_s$ where

DD FORM 1 JAN 73 1473 EDITION OF 1 NOV 65 IS OBSOLETE

SECURITY CLASSIFICATION OF THIS PAGE *(When Data Entered)*

* D sub p = 4 C sub mn to the 2nd power / M sub e C sub s

C_μ is related to lubrication parameters, M_e is the effective cage mass, and C_s is a cage material-geometry parameter. If D_p is less than unity, the cage is predicted to be stable. Conversely, if D_p is greater than unity, an instability should occur.

FOREWORD

The purpose of the program is to investigate cage and bearing instability in despun antenna bearings due to changes in lubricant properties The program is being conducted at Battelle's Columbus Laboratories, 505 King Avenue, Columbus, Ohio 43201, for the Air Force Material Laboratory, under Contract F-33615-74-C-5012. (Project-Task Number 7343 03 16.)

Mr. R. J. Benzing and Dr. Mario Rivera (AFML/MBT) of the Lubricants and Tribology Branch, Air Force Materials Laboratory are the Project Engineers. This report is the first summary report under the contract and covers the period February 1, 1974, to January 31, 1975.

Mr. J. W. Kannel has been the Principal Investigator and has had the overall responsibility of the program. He has been assisted at Battelle by Dr. S. S. Bupara. Most of the experimental work published herein has been conducted by COMSAT Laboratories, at Clarksburg, Maryland, with Mr. Chester Pentlicki acting as subcontractor Project Engineer.

The report was submitted by the authors January 31, 1975.

TABLE OF CONTENTS

LIST OF ILLUSTRATIONS

LIST OF ILLUSTRATIONS (Continued)

LIST OF TABLES

SUMMARY AND CONCLUSIONS

The objective of the program has been to perform analytical and experimental investigations of cage and bearing instability in low-speed, lightly-loaded bearings typified by bearing for despun mechanical systems for satellite attitude control. The analyses are being conducted at Battelle's Columbus Laboratories (BCL). They involve the use of a computer model for the bearing which predicts cage motions as a function of lubricant properties and bearing design. Empirical inputs of lubricant and cage-spring mass properties are used in the analyses to ensure accuracy of the modeling. In addition, experiments are being conducted at COMSAT Laboratories to observe cage motion as a function of design and operating conditions.

The analyses have involved the development of a specialized version of BCL's bearing dynamics program, BASDAP, designated as BASDAP II. BASDAP II is distinguished from BASDAP I in that it uses a series of closed form solutions for in-plane equations of motion of the cage. In the operation of BASDAP II, the motion of the bearing cage is traced as a function of time. Whenever the cage impacts a ball or race, the cage momentum is altered and the cage undergoes a rebounding action. The extent of rebounding, and hence a measure of the energy imparted to the cage, depends on the extent of elastohydrodynamic lubrication of the ball race interface, the viscosity of the bearing lubricant, and the spring rate properties of the cage material. An analysis of the rebounding phenomena has led to the development of a stability criterion (Equation 3).

Two types of experimental evaluations of the BASDAP II model are being pursued. One type involves a qualitative correlation between actual spacecraft observations and predictions obtained from BASDAP II. The results indicate, both from the stability predictions and the experimental observations, that typical despun bearing-lubrication systems operate very near the threshhold of instability; moreover, relatively small changes in the external conditions, such as fluid viscosity, can trigger the instability.

The second type of experimental validation involves operating bearings under various conditions of lubricant quantity, lubricant viscosity and geometric factors and of monitoring stability. Experiments conducted thus far with Apiezon-C at room temperature and a standard flight quality bearing indicate the following.

(1) Stability improves with increasing lubricant quantity for near starvation condition as would be predicted by BASDAP II.

(2) Torque variations are coupled with variations in film thickness as would be predicted by BASDAP II. However, it is not certain at this stage which occurs first.

(3) Some instabilities still occur for adequate lubrication conditions as could be expected by virture of the thin EHD film and high viscosity of the lubricant.

During the second year of the program, a more quantitative comparison between laboratory experiments and BASDAP II calculations will be made. It is anticipated that the experimental data will guide the computer modeling to achieve an accurate evaluation of actual bearing dynamics.

Based on the analytical and experimental work conducted thus far, a stability model for the despun bearing is evolving. During the second year of the program, it is anticipated that this model will be more fully verified and, in addition, that numerous tests and analyses will have been conducted to evaluate despun bearing operation. These evaluations will include effect of lubricant viscosity and bearing geometry factors.

INTRODUCTION

Despun mechanical assemblies (DMA's) are expected to function without relubrication or maintenance for lifetimes of 10 to 15 years in space. In order to define bearing performance and reliability in such systems, it is necessary to understand the failure mechanisms that may result in loss of the ability of the system to perform its mission. Furthermore, the fundamental failure mechanisms must be understood in order that accelerated tests can be developed to evaluate performance life. One type of failure that has been observed in space for DMA's is cage (separator) instability in the ball bearings which has caused abnormal torque variation and serious pointing errors in the antenna. In some instances, these instabilities have occurred shortly after a change in the thermal environment of the bearing has been experienced. Therefore, serious concern exists about the useful life of the satellite if continued deterioriation of bearing performance should occur. In addition, it is possible that increasingly stringent pointing requirements will further increase the demands on the DMA bearing.

In order to develop adequate accelerated life tests for bearings, it is necessary to understand all of the possible failure mechanisms (cage instability has been shown to be an important failure mode) so that separate accelerated tests can be devised and performed for each failure mechanism. Unfortunately, the state of the art is such that an understanding of how cage instability depends on bearing design factors and lubricant properties is not available as yet. In the absence of such an understanding, it is neither possible to design DMA bearings intentionally to be stable, nor to devise accurate life tests to evaluate stability. The objective of this research program is to perform analytical and experimental investigations which are expected to enhance this understanding.

The analyses are being conducted at Battelle's Columbus Laboratories (BCL). They involve the use of a computer model for the bearing which predicts cage motion as a function of lubricant properties and bearing design; this program is based on the computer program BASDAP[1,2] developed earlier by BCL and is called BASDAP II. In addition to the analyses, experiments are being conducted at COMSAT Laboratories to actually measure cage motion as a function of design and operating conditions.

SIGNIFICANCE OF REPORTED RESEARCH

The objective of the research program reported herein has been and is to advance the understanding of cage and bearing instability in despun mechanical assemblies, DMA's, to the extent that life test methodology can be devised. An attractive additional objective is to develop design criteria which will result in the elimination of such instabilities. This document represents the first of two annual reports scheduled for the contract, and summarizes the groundwork performed toward achieving the full objectives of the program. The groundwork has been oriented in such a way that the remaining research efforts will represent practical application of the technology.

In reality, significant strides have been made toward establishing not only a computer program for studying cage instability and associated experimental backup but also toward establishing a stability criterion for the bearing. This criterion, if validated in subsequent work, represents a momentus step forward in understanding not only DMA bearings but also most types of angular contact bearings. The equation for the stability criterion can be written (Equation 3 of the text).

$$D_p = \frac{4C_\mu^2}{M_e C_{s_1}} ,$$

where M_e^* is the effective cage mass, C_{s_1} is the ball-pocket spring constant, and

$$C_\mu = \frac{2A}{h} \mu_i \frac{[e^{\gamma P_h}(\gamma P_h - 1) + 1]}{(\gamma P_h)^2}$$

Here A is the ball race contact area, h is the ball race film thickness and $\mu_i e^{\gamma P_h}$ is the viscosity of the lubricant between ball and race.

If D_p is greater than 1, the cage is unstable. Conversely, if D_p is less than 1, the cage is stable. The bearing dynamics calculations, the laboratory experiments, and spacecraft observations tend to substantiate this criterion for a bearing with a ball-guided cage. However, it must be noted that the criterion is still a preliminary one.

Assuming the validity of the stability criterion, from the point of view of bearing-lubricant design, the DMA designer has several options. He can work toward a large value of h, a small value of μ_i or large value of M_e or C_{s_1}. All of these parameters are reasonable design variables. By considering the criterion from the point of view of life test methodology, the test engineer can accelerate the anticipated lubricant depletion and attendant starvation in the bearing to force premature instability. Likewise, he can evaluate the effect of cage wear on the spring constant. Also, the role of wear debris on viscosity is a possible "failure" related parameter. In general, a stability criterion, if it holds up in subsequent research, allows for the development of a model law for bearing failure.

---

* M_e = 1/2 the total cage mass.

PROJECT ACTIVITIES

The bearings used in DMA's typically are very light, large bore (~100 mm), slow speed (~100 rpm), lightly loaded (~100 lb) bearings, in which normally very viscous lubricants are used to ensure adequate ball-race lubricant films. The cage in the bearing can be a conventional race-guided configuration or a ball-guided configuration of the type shown in Figure 1. Here, a cone surface is located, inboard of the normal cage cylinder, to centralize the cage location. However, since the cage is not physically attached to any other bearing element, its motions are subject to many uncertainties. In many instances, the cage will incur an instability (known as a groan) which causes serious torque fluctuations in the bearing and pointing inaccuracies in the DMA. The purpose of the research presented here has been to elucidate these instabilities so that test methodology can be developed to evaluate long-term bearing performance.

The specifications used for the antenna bearing study are given in Table I. These specifications were selected by mutual agreement between BCL, AFML, and COMSAT. This bearing represents a typical bearing for a DMA and is a bearing with a known propensity for instability.

DESCRIPTION OF BASDAP II

The computer program BASDAP represents a very complex and generalized program for the evaluation of cage dynamics in a bearing. In the BASDAP computer program, the cage, itself, is treated as a 6 degree of freedom rigid rotator. This computer program has been used in a variety of research programs including antenna bearing studies. However, the computing-time requirements to obtain a convergent solution are quite long and some improvements in the numerical scheme are in order to make it a more useful tool for detailed bearing dynamics studies.

The numerical technique used in BASDAP involved a fourth order Runga-Kutta numerical scheme for the integration of the equations of motion for the cage. This involves, then, a point by point numerical integration of the equations and requires time steps on the order of 10^{-6} - 10^{-7} sec increments to obtain convergence. The basic approach for simplifying the program, is to obtain closed form solutions to the equations for at least a portion of the cage motion. This simplified computer program is known as BASDAP II.

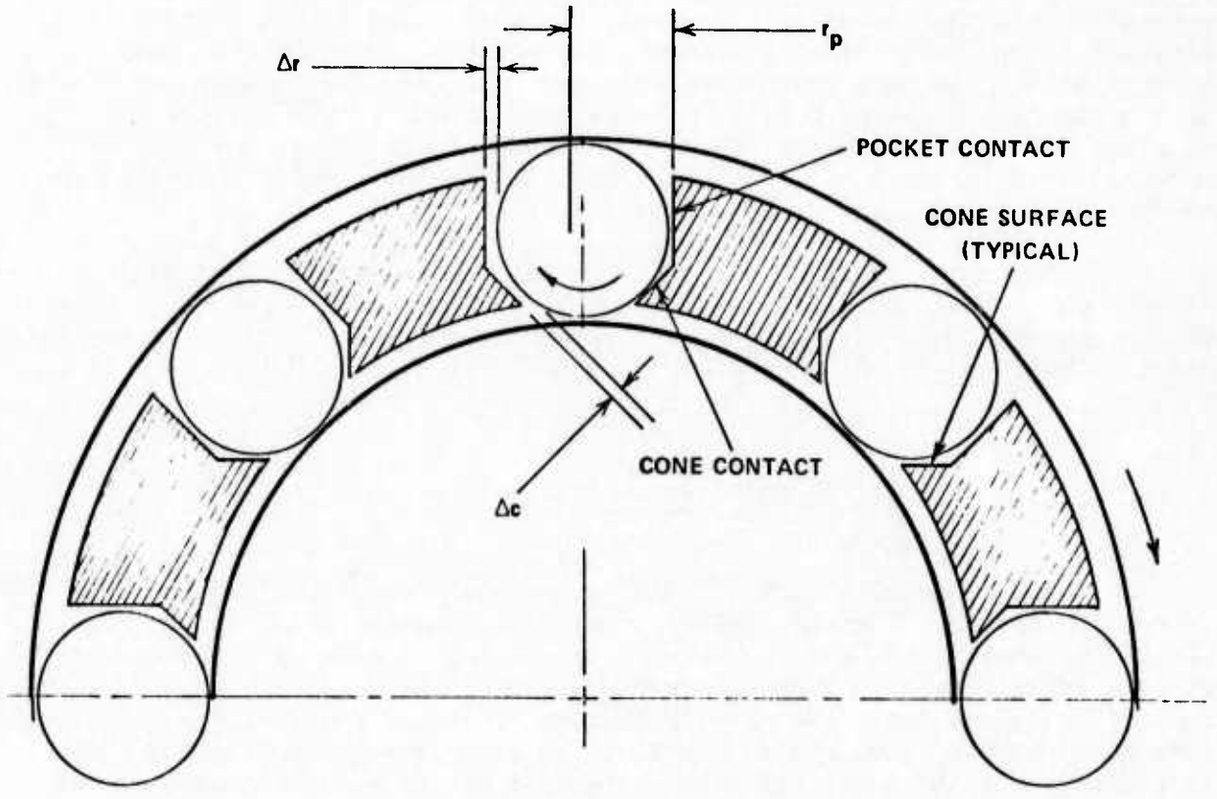

FIGURE 1. GEOMETRY OF BEARING ANALYZED

TABLE I. SPECIFICATIONS USED FOR ANTENNA BEARING COMPUTER STUDY

Parameter	Numerical Value
Number of balls	16
Ball diameter, in.	0.59375
Ball mass, lb	0.022
Separator mass, lb	0.125
Separator pocket diameter, in.	0.6130
Outer-race curvature, percent	52.5
Inner-race curvature, percent	52.0
Bore diameter, in.	3.543
Pitch diameter, in.	4.52765
Contact angle, degrees	26.14
Cone angle, degrees	67.5
Axial thrust load, lb	60
Shaft speed, rpm	60

Approach for BASDAP II

Consider the bearing of Figure 1. Assume that the cage starts in motion in any direction. This motion will continue until the cage-pocket impacts a ball either on the cone or on the pocket. During the impact, the rotational motion of the ball will impart a momentum to the cage in the direction of rotation. In addition, under some conditions, the cage will bounce off the ball so that the resultant motions of the cage will tend to be away from and radially inward (when the cage hits the front of the ball as shown in Figure 1) or outward (when the cage hits the back of the ball). If the cage were race guided (i.e., if it contained no cone surface), then the cage could also, under some conditions, impact and bounce off the race.

It is apparent, then, that the motions of the cage depend heavily on the spring characteristics of the cage-ball or cage-race interface, on the damping of the motions due to the ball slippage on the races, and on the friction force at the contact interfaces. A usable analytical model for the bearing, then, must account for each of these factors in a realistic manner. And, in addition, the model must relate these factors to the momentum transferred to the cage. With a knowledge of these momentum transfer forces, the equations of motion of the cage can be solved.

The sequence for the solution to the cage motions is as follows.

(1) The center of mass motion of the cage (in the absence of ball-cage contact) is computed by, whenever possible, a closed form solution.

(2) The cage rotational motion (in the absence of ball-cage contact) is computed by a closed form solution.

(3) The ball-pocket orientation for each ball is scanned at each time step to determine the onset of ball-to-pocket contact.

(4) At contact, the impact equations are solved by a closed form solution and the impulse transmitted to the cage is determined. The sequence is now repeated for a large number of time increments and the forces on the cage and the cage dynamics are traced as a function of time.

Block Diagram of BASDAP II

A block diagram for the BASDAP II computer program is shown in Figure 2 and described below. Two appraoches are used for Blocks 1 through 3. The current approach is to compute these inputs (exclusive of the spring constants) separately and to input them into BASDAP II, though a more general program has also been developed.

Block (1) Input Bearing Design Parameters

This block sets the basic parameters for the bearing. This includes the design contact angles, the bearing speed, the lubricant viscosity including pressure-viscosity effect, and the bearing geometry.

Block (2) Statics Analyses of Contacts

Using the theory advanced by A. B. Jones [3], the contact pressures between balls and races are computed as are the contact areas and contact angles. These analyses are described in Appendix A and represent an elasticity balance and allow for radial loadings, as well as axial loadings. Centrifugal ball loadings are also inherent in the computations -- though they are insignificant for a DMA bearing. Finally, these analyses can include the computation of individual ball velocities due to contact-angle variations.

Block (3) EHD Films and Spring Constants

The lubricant film at the ball-race contacts are computed using the BCL empirical film-thickness equation[4]. These calculations utilize the contact stresses and velocities developed in Block (2). Finally, three constants discussed in Appendix B are computed. These are

C_μ ~ The ball-race traction constant

C_{s_1} ~ The ball-pocket linearized spring constant

C_{s_2} ~ The cage-race spring constant .

Block (4) Initialize the Cage Position and Velocities

The coordinate system for the cage analysis is given in Figure 3. The primary coordinates and their time-derivatives for the in-plane analyses are as follows

ρ = The displacement of the center of mass relative to the geometric center of the bearing

β = The angular location of the center of mass

α = The reference angle through which the cage has rotated.

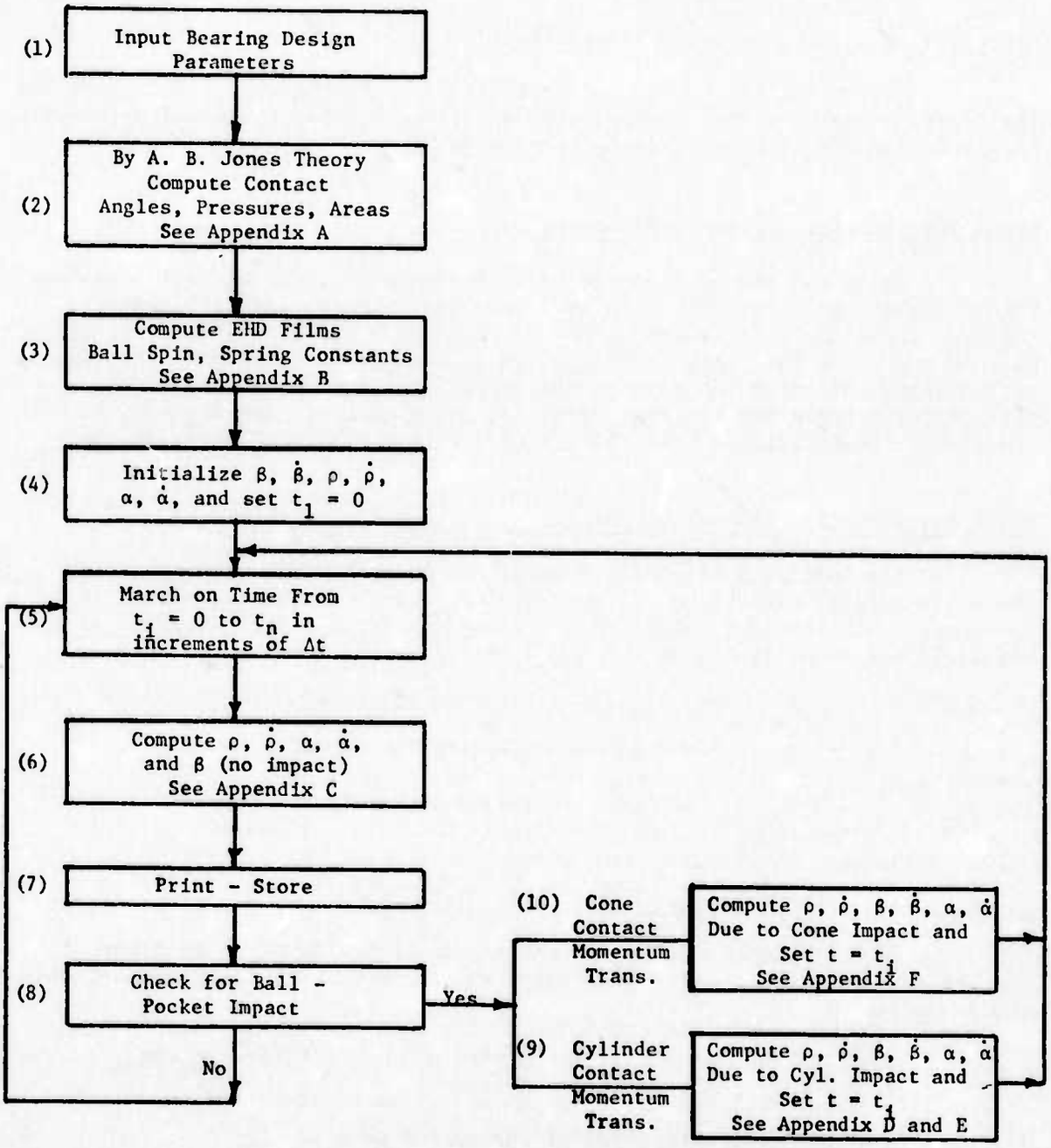

FIGURE 2. BLOCK DIAGRAM FOR BASDAP II PROGRAM

The time record t_1 is set initially at 0.

Block (5) Time Sequencing for Cage Dynamics

Time, in the absence of ball-pocket impact, is sequenced. Whenever Block (5) is entered via Blocks (9) or (10), the incremental time sequence is rezeroed. However, a continuous record of the total time is maintained.

Block (6) Computation of α, $\dot{\alpha}$, β, $\dot{\beta}$, ρ, and $\dot{\rho}$ (No Ball Impact)

CM Radial Motion and Displacement ($\dot{\rho}$ and $\dot{\rho}$). The center-of-mass of the cage can oscillate radially through a maximum of $2\rho_m$, where ρ_m is the radial clearance between the cage and race, without contacting the race. For the case where $\rho < \rho_m$ and there is no ball-cage impact, the only external force on the cage is that due to centrifugal loading due to $\dot{\beta}^2$. Conversely, for a ball-guided cage, when $\rho > \rho_m$, the cage contacts the race and a spring-type force is applied to the cage. The equation of motion for ρ, then, depends on which of these two conditions is extant at any particular time.

A special subroutine has been developed which computes the changes in the value of ρ and $\dot{\rho}$ through any time increment. The analyses for this subroutine are given in Appendix C.

With the use of Equations C-1 through C-9, it is possible to compute the location and velocity vectors for the cage CM for any time increment. In the operation of the computer program, the subroutine is supplied values of ρ_i and $\dot{\rho}_i$, as well as a series of functions which are assumed not to vary during the time increment Δt. The computer seeks the appropriate equation (i.e., Equations C-3 and C-5) and the time that this solution is active, e.g., t_a. If t_a is less than Δt, the computer switches equations at the end of t_a and repeats the logic. This progress is continued until the CM is traced throughout the entire Δt increment. The method for tracing the CM motion represents a quasi closed-form technique as opposed to a finite-difference solution, since it utilizes an actual solution to the motion equation. Thus, the subroutine is not subject to the same numerical idiosyncrasies inherent in finite-difference techniques.

Cage Rotation (α and $\dot{\alpha}$)(No Impact). In the absence of ball contact, the only constraint as the cage rotates is associated with the friction force at the guiding surface when $\rho > \rho_m$. In the computational techniques, this frictional force is assumed to be constant throughout the time interval. With this assumption, it can be shown that

$$I\dot{\alpha}^{\cdot} = (R_c - R_p)\, F_f \,, \tag{1}$$

where I is the mass moment of inertia, F_f is the frictional force and $(R_c - R_p)$ is the radial location of the frictional force relative to the center of mass (see Figure 3). Equation 1 can be readily integrated to yield α and $\dot{\alpha}$ as a function of time.

Block (7) Store and Print

The dynamics computer program is constructed such that the pertinent printouts will be made as they are generated. However, to minimize the amount of output, these printouts will contain only the pertinent variables such as the value of cage location vectors (to assess stability) and the ball-cage contact forces. In addition, the data are stored to allow for direct computer plotting.

Block (8) Status of Ball-Pocket Contact

Each ball will orbit the bearing center at some angular velocity, $\dot{\alpha}_B(n)$ (see Figure 4), dependent, primarily, on the contact angles. At some condition, the angular position of the cage, α, will be such that ball-pocket contact will occur. The condition promoting impact is described in Appendix D, Equation D-1. This impact condition is related to

(a) The rotational angle of the cage

(b) The center of mass location of the cage.

Block (9) Momentum Transfer at Ball-Cage Impact

As discussed in the approach section, a rebound motion of the cage will occur following ball-cage impact. This rebound is related to the spring-rate of the ball-pocket interface and the viscous resistance of the ball-race interface. In simplified form, it can be stated that the relation between the rebound velocity and the impact velocity is given by

$$u_o = -eu_i \ , \qquad (2)$$

where u_i is the impact velocity of a point on the cage with the ball and e is a constant of restitution which is related to spring rate, viscosity, etc. Referring to Appendix E, the value of e will be 0 if $D_p < 1$, otherwise it will be the value given by Equation E-6.

In order to determine the effect of impact on cage motion, it is necessary to transform the cage velocity coordinates ($\dot{\alpha}$, β, and $\dot{\beta}$) into effective values of u_i and v_i and, following impact, it is necessary to transform the value of u_o and v_o back into cage velocity coordinates. These transformations are given in Appendix D, and consist of the following steps.

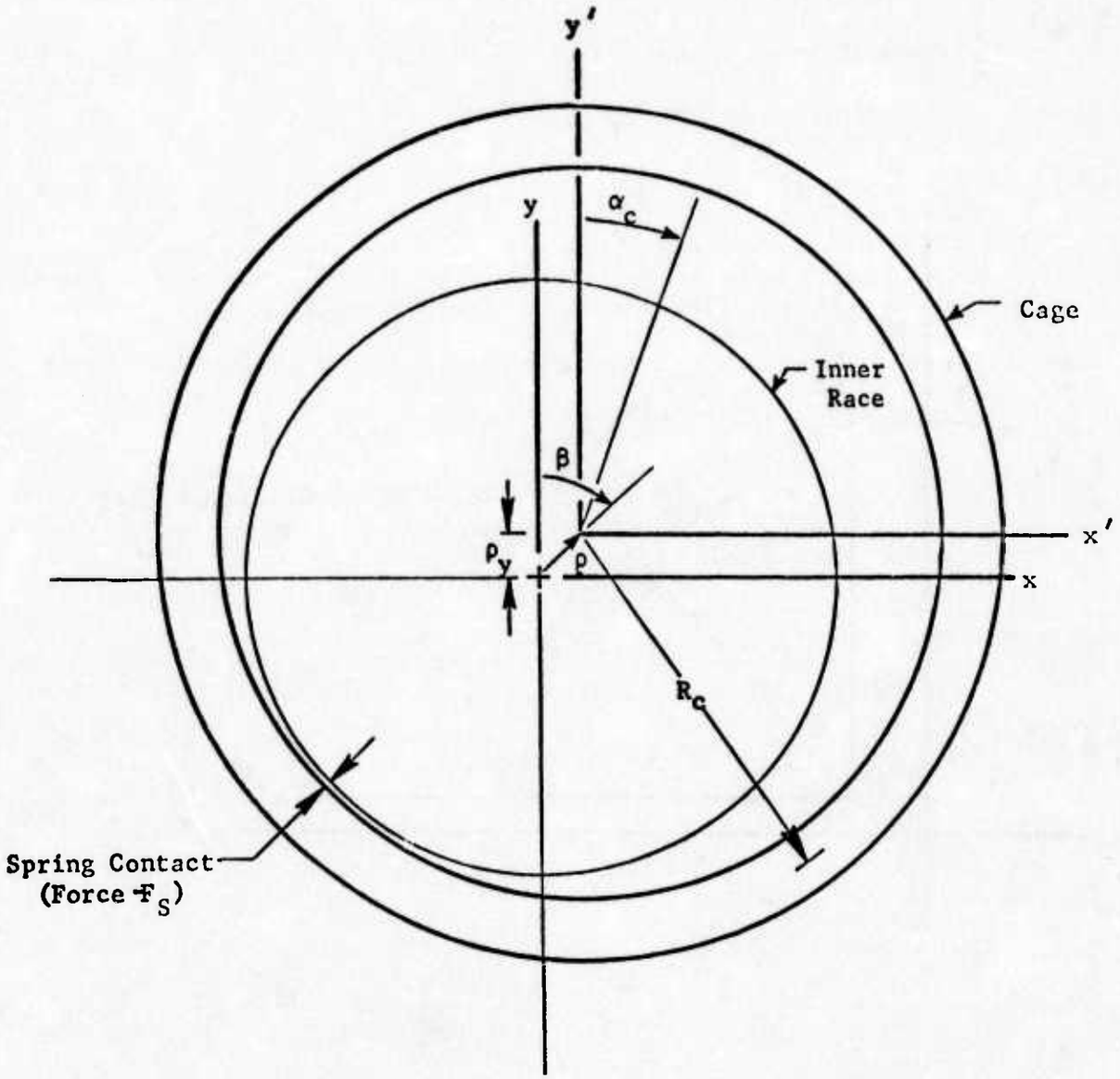

FIGURE 3. COORDINATE SYSTEM FOR INPLANE CAGE ANALYSES

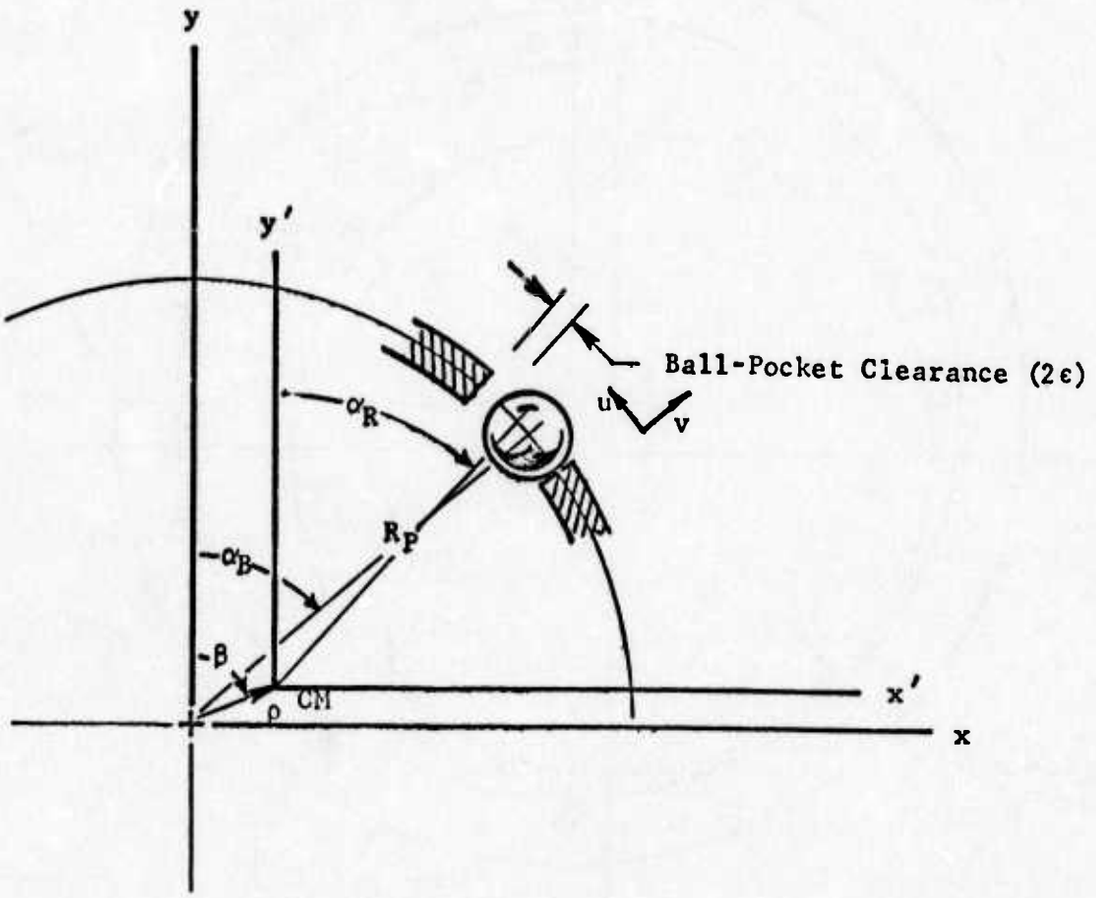

FIGURE 4. COORDINATE SYSTEM FOR CAGE-BALL LOCATIONS

(1) The value of $\dot{\beta}$ and $\dot{\rho}$ at the time impact first occurs are transformed into rectangular velocity coordinate for the cage CM, $\dot{x}$ and $\dot{y}$ (Equation D-2).

(2) The value $\dot{x}$ and $\dot{y}$ from Step 1 along with the initial value of $\dot{\alpha}$ are transformed into values of u and v (Figure 4) for the particular pocket incurring impact (Equation D-3).

(3) The value of u_o is now computed by Equation 2 and v_o is computed by Equation D-9.

(4) The values u_o and v_o are transformed into the rectangular velocity components $\dot{x}$ and $\dot{y}$ for the center of mass (Equation D-10)

(5) Finally, the values of $\dot{x}$ and $\dot{y}$ are transformed into the new values of $\dot{\alpha}$, $\dot{\beta}$, and $\dot{\rho}$.

In the appendix, the prime superscript refers to the CM coordinates and the o and i subscripts refer to rebound and impact conditions, respectively. The value of the velocity coordinates $\dot{\alpha}$, $\dot{\beta}$, and $\dot{\rho}$ after rebound are fed into the Block 5 of the computer program (Figure 2) and the time cycle repeated until a preset number of total time step have been incurred.

A similar procedure is used if ball-cone contact occurs. The equations for this type of contact are discussed in Appendix F.

COMPUTATIONS USING BASDAP II

Empirical Inputs

The success of any analytical modeling of a complex system such as a ball bearing, depends heavily on the validity of the specific modeling of each subcomponent in the system. Two inherent assumptions used in the BASDAP program are:

(1) The ball race interface is modeled as a lubricated contact where the tractions are modeled by bearing elastohydrodynamic (EHD) lubrication theory.

(2) The ball cage and cage-race interfaces are representative of a dry spring interface whence the normal forces are modeled by a spring constant and the traction forces are modeled by a coefficient of friction.

In order then to ensure realistic BASDAP calculations, these models have been evaluated experimentally and also empirical numbers have been used for inputs.

Empirical Evaluation of Ball-Race Interface

The primary factor controlling the frictional forces at the ball-race contact is the viscosity of the lubricant in the contact zone. The lubricant used for the analysis was Apiezon-C (94.3 cs at 100 F and 10.1 cs at 210 F) containing an E.P. additive. A technique using a pair of rolling disks[5] was used for the rheology evaluations of this lubricant.

The rolling-disk (or cylinder) viscometer is shown schematically in Figure 5. Two 1-inch diameter disks (containing a 16-inch crown radius) are loaded together into lubricated (5000 rpm) rolling contact to the contact-pressure levels of interest (100,000 to 200,000 psi). Slippage is introduced between the disks and measurements of the slip rate and the contact-zone tractive force are made. The tractive force is measured with use of a load cell which constrains the upper unit, and slippage is determined by measuring, independently, the speed of each disk with electronic counters in conjunction with magnetic pickups. With the apparatus, traction versus slip curves are obtained for various levels of contact pressure.

Several traction curves as obtained using Apiezon-C as the lubricant[2] and are presented in Figure 6. The low-slip portions of the curves are essentially linear, which implies a linear proportionality between the shear stress and shear rate in the lubricant. By analyzing this linear portion, inferences about lubricant viscosity can be made. The pressure-viscosity curve so obtained for Apiezon-C is given in Figure 7. Under the pressure condition of interest (>70,000 psi), the viscosity of this lubricant is very high (of the order of 10^6 centipoise). As will be discussed later, this high viscosity can cause extreme stiffness at the ball-race junction which, in turn, can cause high forces to occur in the bearing, notably between the ball and separator. Also, given in Figure 7 are pressure viscosity data[6] for Vackote obtained by standard viscosity measurement.

Empirical Evaluation of Ball-Cage Interface

Ball-Cage Spring Rate. An analytical expression, based on theory of elasticity, for ball-cage spring rate, C_s, is given in Appendix B. To evaluate this spring constant, some experiments have been conducted. These experiments involved loading a segment of the cage pocket against a ball and of measuring the interface deflection characteristics. The results of these experiments are given in Figure 8. As can be observed, surprisingly good modeling of C_s has been achieved analytically. This value can be further improved by using a value of E_c of 0.8×10^5 rather than 10^5 psi.

Ball-Cage Frictional Forces. The measurement of ball-cage frictional forces is discussed in Reference 2. In those measurements, a segment of an actual separator was loaded against the ball in the pocket region with a hinged loading arrangement. The friction force was measured by means of four strain gages bonded to a thin cantilever beam. Data were obtained using phenolic separators having three levels of porosity (0.2 percent, 4 percent, and 27 percent), as supplied by COMSAT Laboratories. The results of the ball-separator friction evaluations are summarized in

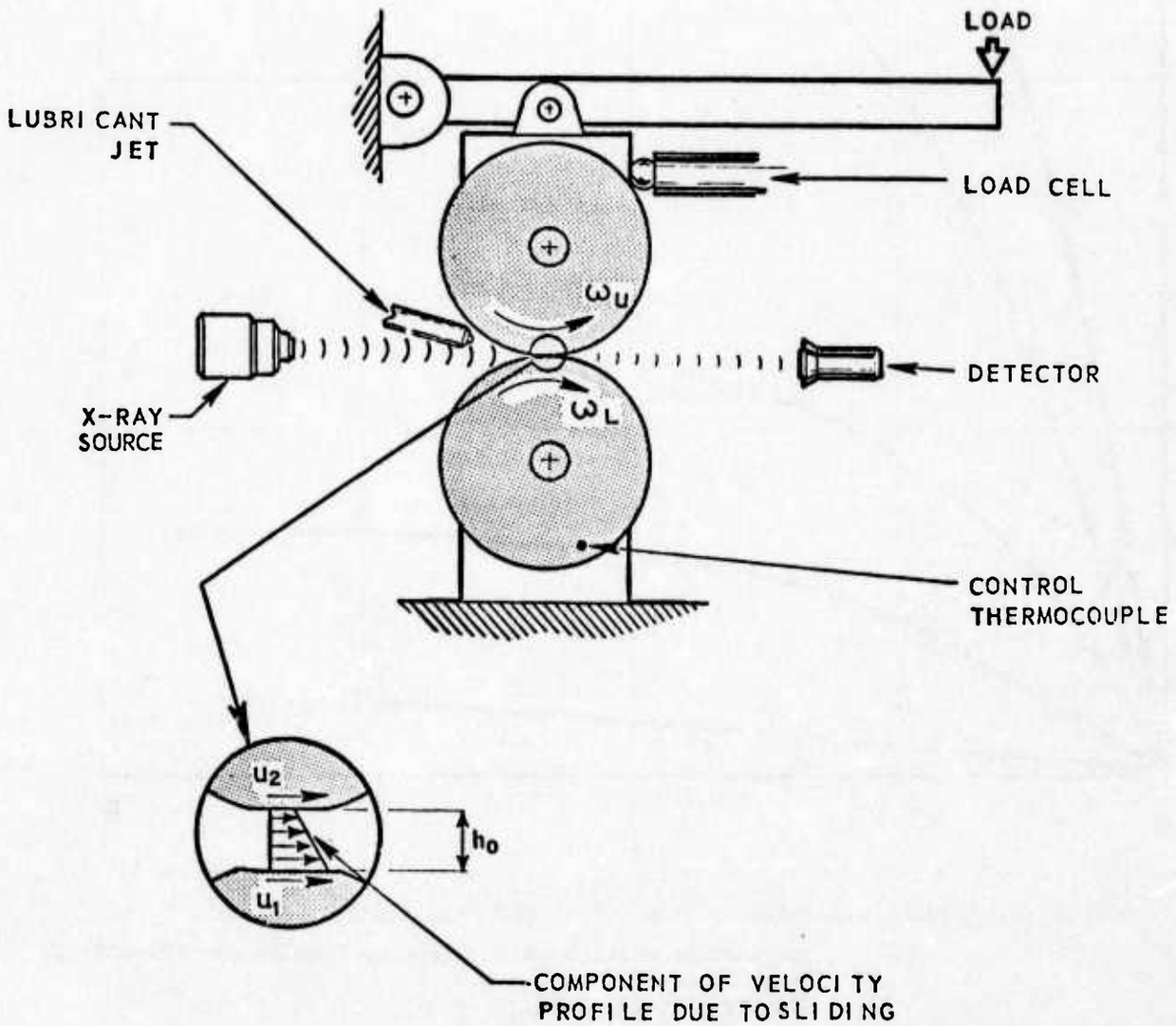

FIGURE 5. ROLLING-DISK RHEOMETER

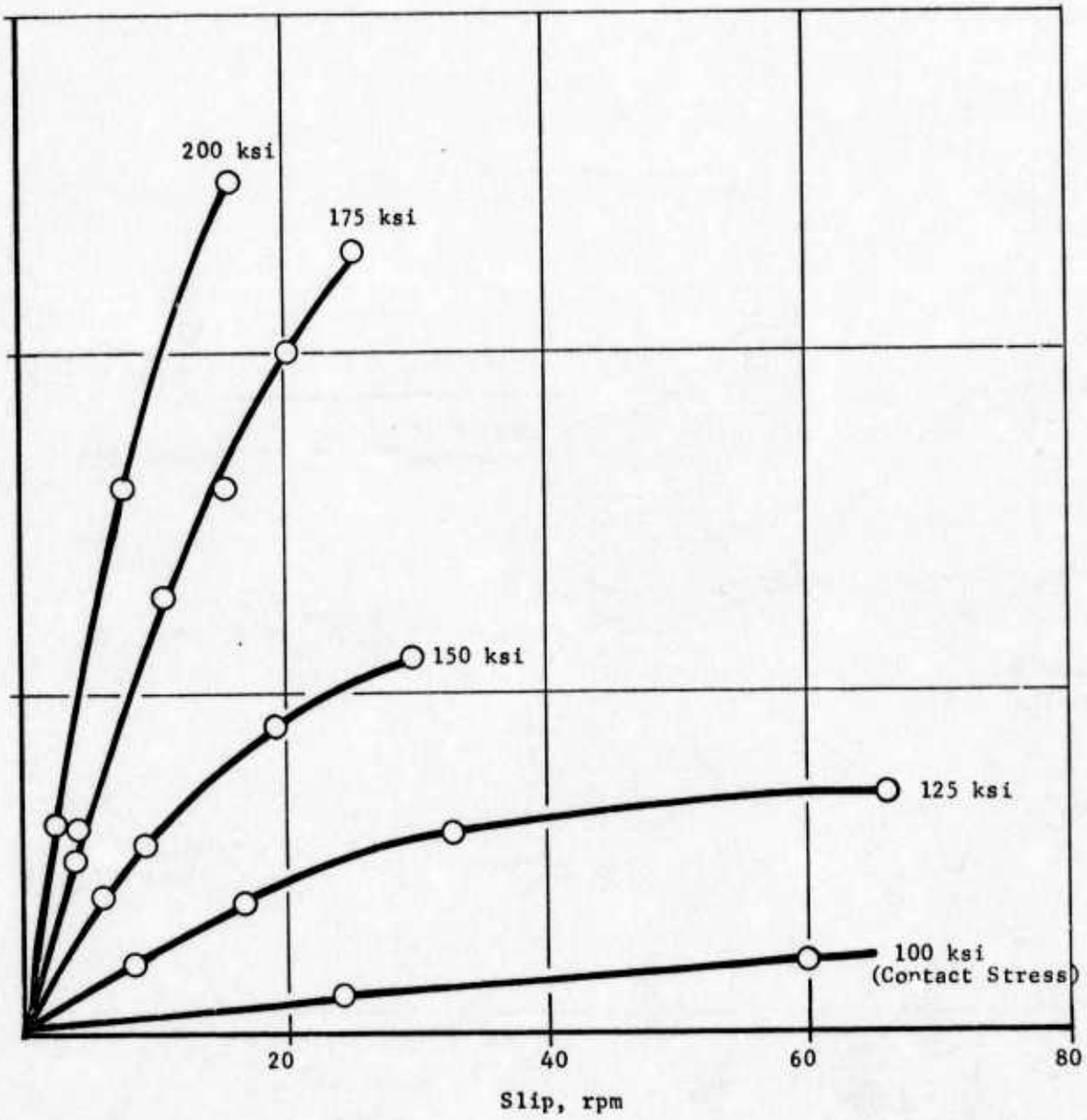

FIGURE 6. TRACTION VERSUS SLIP DATA FOR APIEZON-C

For various Hertz Contact Pressure Conditions (100-200 ksi)
1-in.-diameter disk
5000-rpm rolling speed

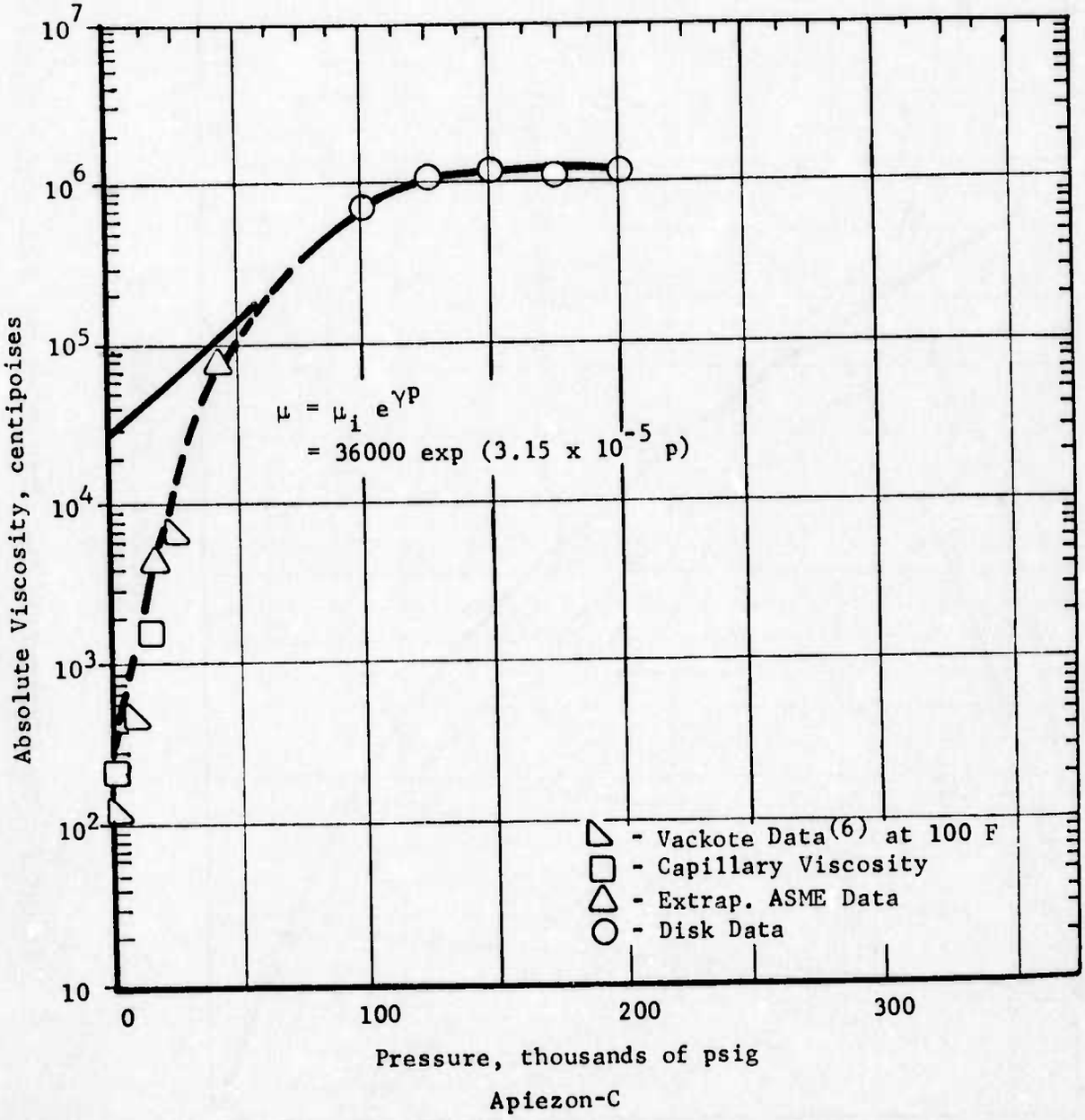

FIGURE 7. PRESSURE-VISCOSITY DATA FOR APIEZON-C

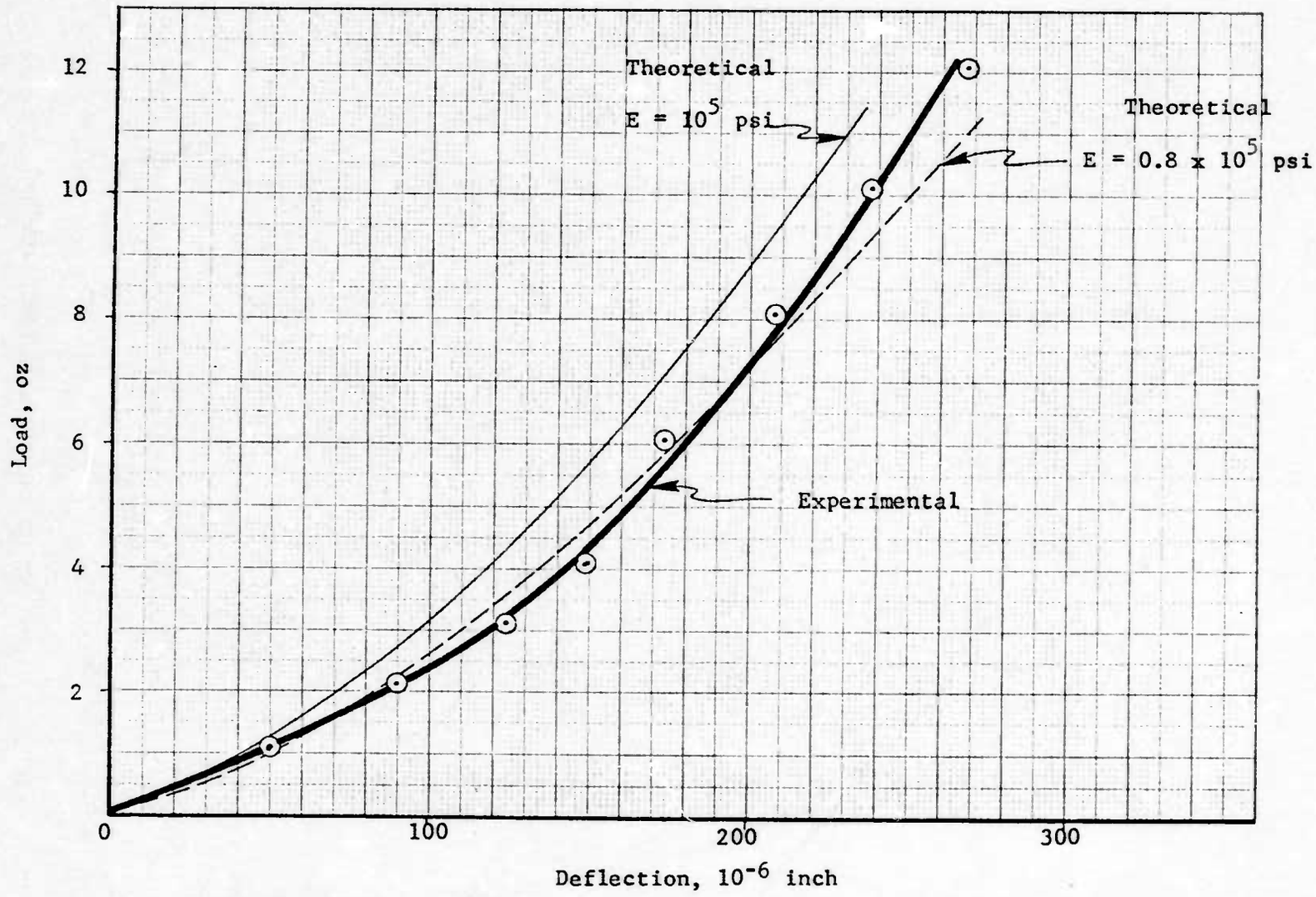

FIGURE 8. LOAD DEFLECTION CHARACTERISTICS FOR BALL-POCKET INTERFACE

Table II. For the cage having a 0.2 percent porosity, experiments were conducted with and without oil impregnation. In all cases, it can be observed that high (and nearly constant) coefficients of friction were observed. The data also indicate that friction in the presence of a lubricant is as high as that experienced in dry contact. The values ranged from 0.2 to 0.4 and increased with increasing porosity. These high values for friction imply that the attendant large normal forces between ball and separator can result in high tangential forces which might affect cage stability.

TABLE II. DATA FOR BALL-CAGE FRICTION[2]

Load, oz	4% Porosity Cage, Standard Lubricant	0.2% Porosity Cage, No Lubricant	0.2% Porosity Cage, Apiezon C Lubricant	27.1% Porosity Cage, Apiezon C Lubricant
0	0.33[a]	0.25	0.23	0.46
1/2	0.33	0.25	0.26	0.41
1	0.30	0.24	0.25	0.41
1-1/2	0.29	0.24	0.23	0.38
2	0.28	0.22	0.23	0.36
3	0.27	0.22	0.21	0.36

(a) Table entry is the dynamic coefficient of friction.

Preliminary Computations with BASDAP II

Computer Runs

The primary efforts thus far in the research program have involved the development of the simplified bearing dynamics program, BASDAP II and preparation of empirical inputs. In essence, this program computes in-plane cage motion using basically a closed form integration scheme for the equation of motions. The program can be used to evaluate both a ball guided and a race guided cage. In addition, two specific cases were evaluated for a ball guided configuration, one case involved using a value of lubricant viscosity that produced high ball-race tractions, whereas the second case involved low ball-race tractions.

Graphs of the prediction of cage oscillation, $\dot{\alpha}$, versus time are given in Figure 9 for a short period of bearing operation. At 0.0149 sec the high traction case produced intolerable $\dot{\alpha}$ motions which aborted the computations, (i.e., the equations predicted cage instability). Conversely,

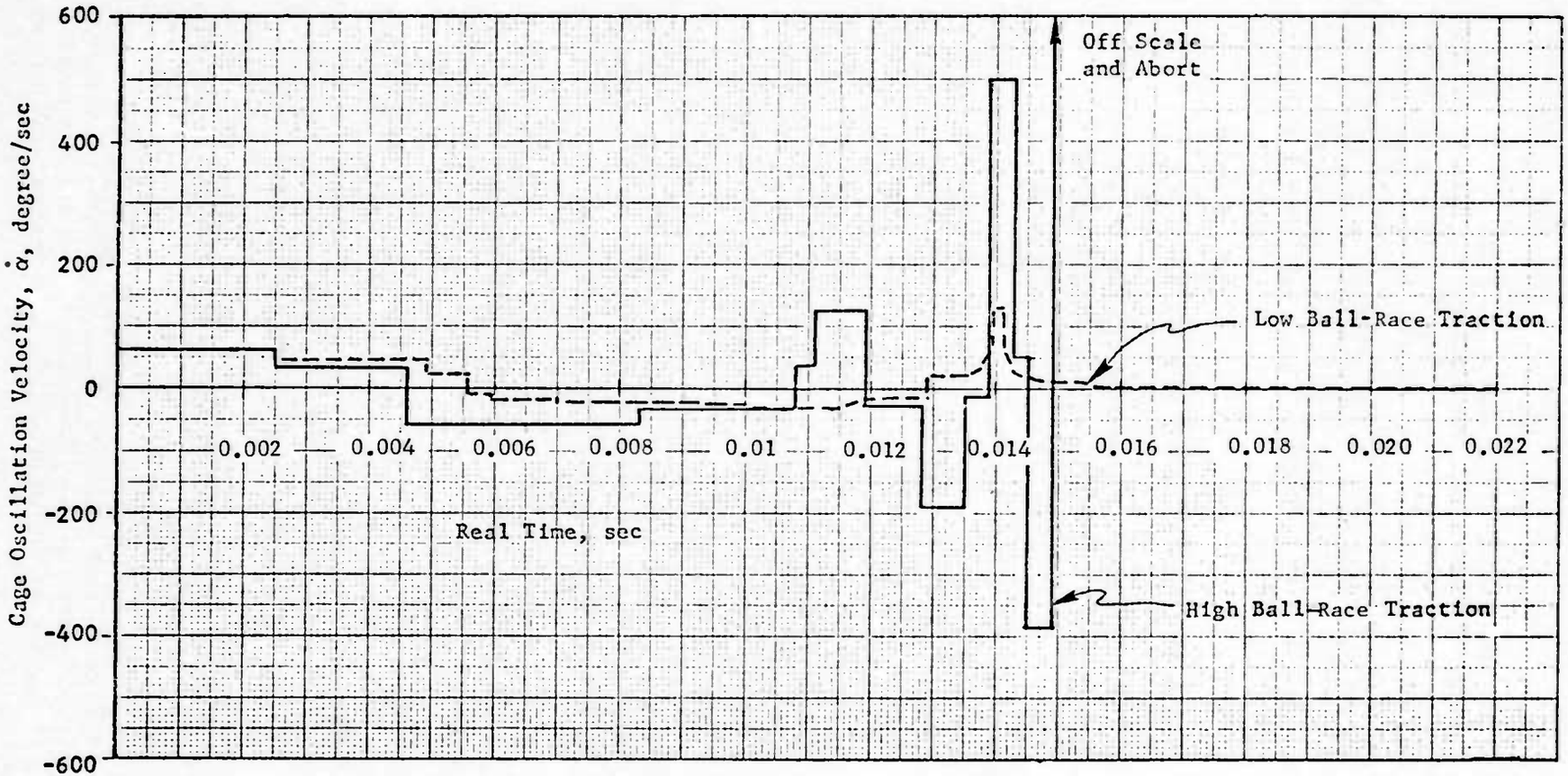

FIGURE 9. CAGE OSCILLATION AS A FUNCTION OF TIME FOR TWO LEVELS OF BALL-RACE TRACTION

for the low traction case, the $\dot{\alpha}$ diminished toward zero after about 0.016 sec of real time indicating definite stability of the predicted cage motion. Mechanistically, then, the viscosity of the lubricant at the ball-race contact is essentially responsible for the damping of the cage motions. That is, high viscosity (i.e., high tractions) causes the cage to bounce off the ball whereas low viscosity causes the ball to absorb the cage motions.

The prediction given in Figure 9 is extremely interesting. If in further evaluations they are found to be realistic, then a real understanding of cage instability is evolving. As discussed in the subsequent section, this stability criterion should be subject to "model" laws which can be used to evaluate cage design concepts as well as life test methodology for cage instability.

Stability Criterion

One advantage of the type of computer technique used for BASDAP II (as opposed to the Runga-Kutta integration of the equation of motion used in the original BASDAP), is that it is possible to determine what aspect of the computer model is triggering an instability. The two cases discussed in the preceding section involved evaluations of low and high ball-race tractions. These tractions only affect the BASDAP II calculations through Equation E-4 of Appendix E. This equation appears in the form

$$D_p = \frac{4C_\mu^2}{M_e C_{s_1}} \quad , \tag{3}$$

where M_e is effective cage mass, C_{s_1} is the ball-cage spring constant (from Appendix B and the preceding section) and C_μ is a viscous term for the ball race interface (also discussed in Appendix B).

If D_p is greater than 1, the cage will "bounce" off the ball and the cage will have a propensity to instability. Conversely, if D_p is less than 1, the cage motion will be absorbed by the ball and the cage will tend to be stable.

EMPIRICAL EVALUATION OF BASDAP II

The credibility of the bearing dynamics model depends on

(1) How well the computer output results correlate with actual space-bearing operation.

(2) How well the output data correlates with the results of laboratory-controlled experiments.

BASDAP Evaluation of Spacecraft Bearings

Cage instability in actual DMA's has been detected by accelerometers attached to the spacecraft. During such instabilities the normal 60-80 Hertz wobble noise of the cage deteriorates into an audible groan from the bearing. Such cage behavior has been seen in laboratory tests, in preflight tests of spacecraft hardware and, as mentioned above, in actual space operation. A cure for the bearing groaning, in space, has been to increase the bearing cavity temperature from the nominal 70 F to around 100 F. One check of the bearing dynamic calculations then would be to compare stability prediction for the two temperature situations. This was done for the case where the lubricant is Apiezon-C and the bearing is the one described in Table I.

Typical condition for a spacecraft bearing for the two temperatures are summarized in Table III. As evidenced by the value of D_p, the bearing conditions are very close to the stability threshhold. Note that D_p can realistically vary widely on either side of unity depending on bearing conditions. The stability criterion for BASDAP II, thus appears to predict very reasonable conditions for a flight bearing.

TABLE III. STABILITY ANALYSIS FOR FLIGHT BEARINGS

Parameter	Units	Case A	Case B
Temperature, T	F	70	120
Lubricant Base Viscosity, μ	cs	250	60
Lubricant Intercept Viscosity, μ_i	cp	3.6×10^4	0.9×10^4
Pressure Viscosity Exp, γ,	psi^{-1}	$3.15\ 0.10^{-5}$	$3.15\ 0.10^{-5}$
Hertz Pressure, P_h	psi	78,000	78,000
Contact Area, A	10^{-4} $in.^2$	1.73	1.73
Effective Cage Mass, M_e	$lb \cdot sec^2/in.$	3.2×10^{-4}	3.2×10^{-4}
EHD Film Thickness, h	10^{-6} in.	10.0	4.0
Ball-Cage Spring Rate, C_{s_1} (linear)	lb/in.	2×10^3	2×10^3
Ball-Race Damping, C_μ		0.54	0.33
Damper Parameters, D_p		1.82 (Unstable)	0.7 (Stable)

Laboratory Evaluations of BASDAP

Most of the experiments are to be conducted by COMSAT Laboratories using flight equivalent bearings. These experiments are to involve measurements to assess the stability characteristics of the bearing under various conditions of lubrication and for various type of configurations. The measurements will include

(1) Dynamic torque fluctuations.

(2) Extent of ball-race EHD lubrication films using an electrical conductivity technique. That is, a voltage is imposed across the bearing and the interruptions to that voltage to metallic contact through the EHD film is observed.

(3) Some actual cage motions.

Effect of Lubricant Quantity on Stability

Two types of experimental series are being conducted to validate the analysis. One experimental series is being conducted to evaluate the propensity of the cage to become unstable as a function of lubricant quantity in the bearing. The second series of experiments will be conducted using a homologous series of lubricants (such as the Kendall SRG series) to establish the effect of viscosity on instability. A minimum of two lubricants will be used, including Vackote. The exact experiments will depend on the data developed.

Some preliminary data have been generated in the oil quantity experiment. The experimental sequence for these tests is as follows.

(1) The bearing is operated dry and the torque behavior measured for 100 rpm motion, 60-lb load, and at room temperature.

(2) Two drops of lubricant (Apiezon-C) are injected into the bearing on two balls 180 degrees apart. Each drop weighs approximately 4 mg and is a mixture of 20 percent oil and 80 percent Freon. Torque and EHD films are then monitored as function of time for several minutes.

(3) Additional quantities of oil are added to the bearing and the EHD film and torque behavior noted.

Typical strip chart recordings of bearing behavior are given in Figures 10 through 13. (Charts are shown in increasing degree of lubrication as outlined in 1 through 3 above.) It can be observed that there is a definite tendency of the bearings to stabilize as lubricant is added.

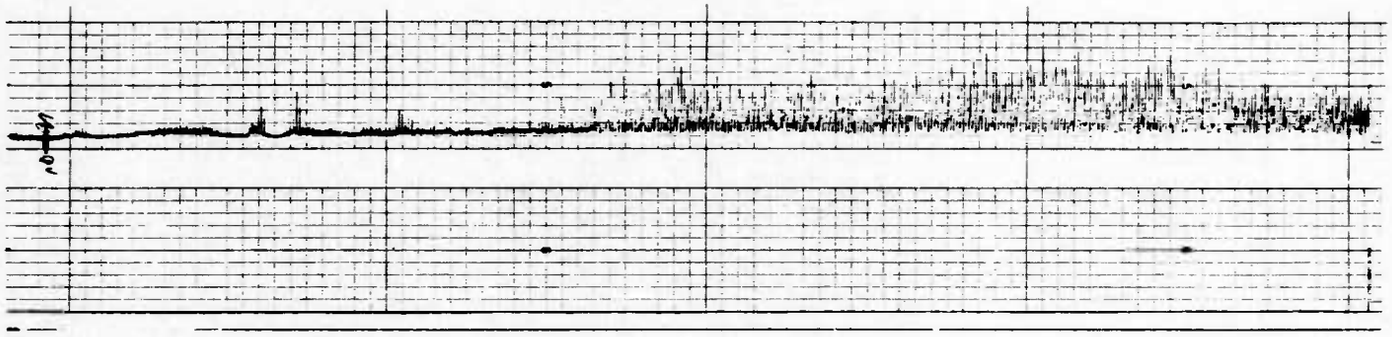

(a) Dry Bearing
Chart Speed 1 div = 5 sec (left to right).

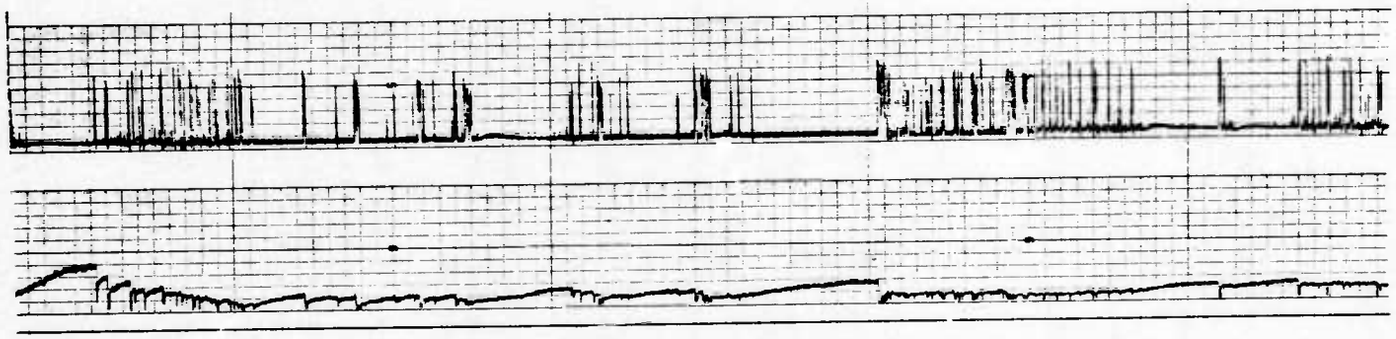

(b) Two Drops of Oil in Bearing
Chart Speed 1 div = 5 sec (left to right).

FIGURE 10. BEARING TORQUE AND FILM THICKNESS MEASUREMENT WITH NO LUBRICANT AND MEAGER LUBRICANTS
(Note: Torque spikes imply instability.)

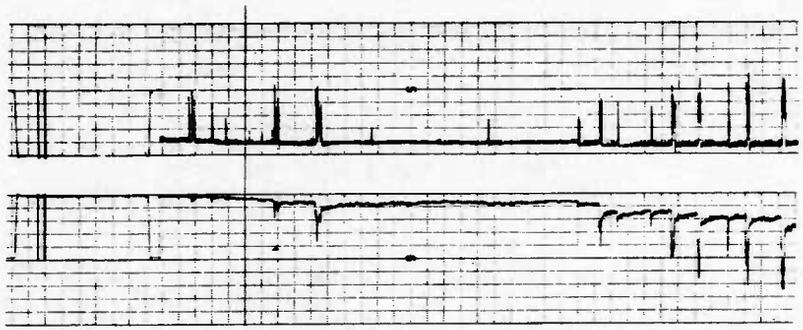

(a) Chart Speed ~ 1 div = 5 sec.

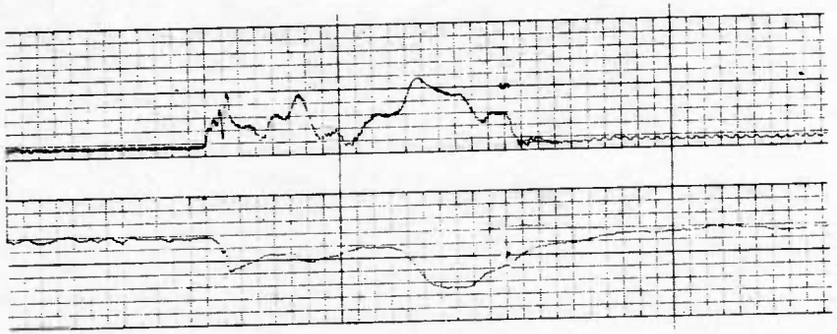

(b) Chart Speed ~ 1 div = 1 sec.

FIGURE 11. BEARING TORQUE AND FILM THICKNESS MEASUREMENT WITH FOUR DROPS OF LUBRICANTS
(Note: Torque spikes imply instability.)

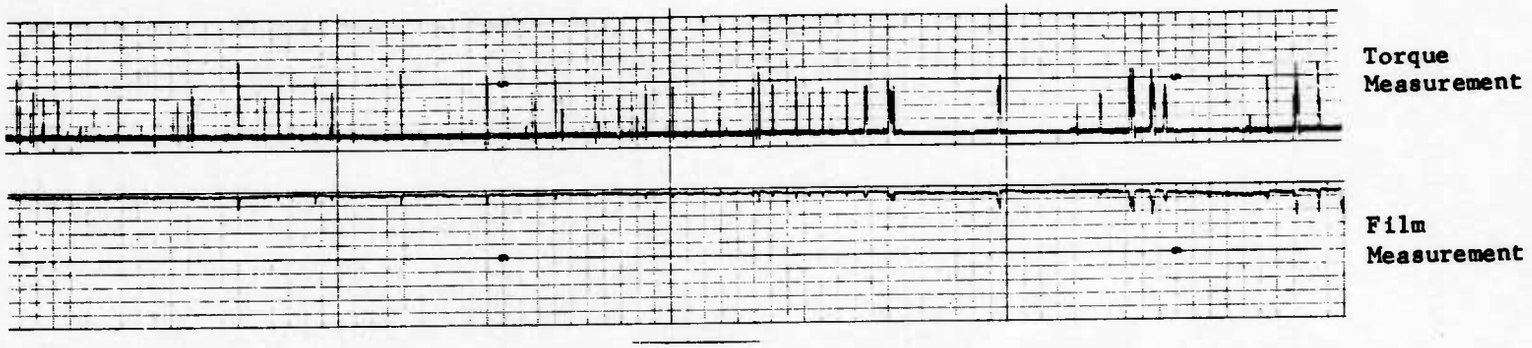

(a) Six drops of oil in bearing.
Chart Speed ~ 1 div = 5 sec.

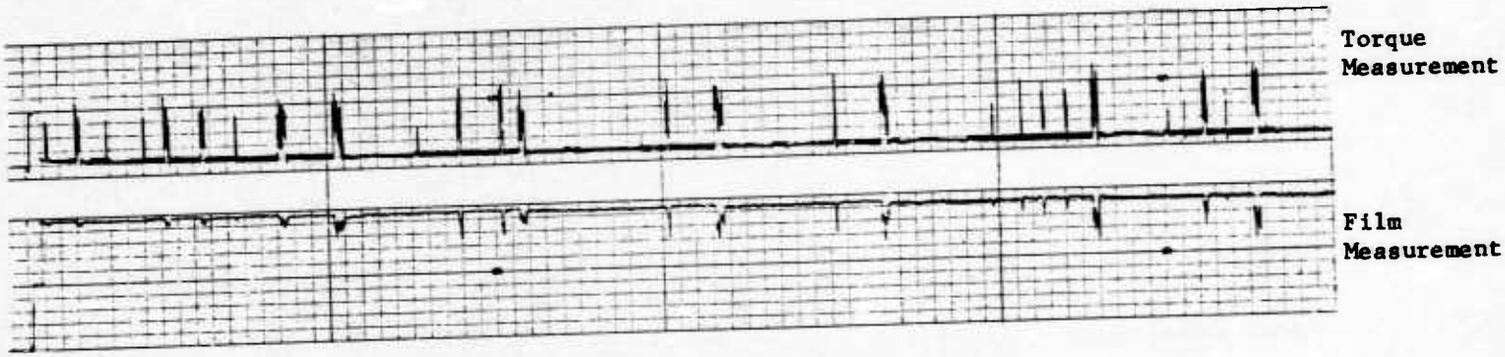

(b) Eight drops of oil in bearing.
Chart Speed ~ 1 div = 5 sec.

FIGURE 12. BEARING TORQUE AND FILM MEASUREMENTS WITH "NEAR ADEQUATE" LUBRICANTS

(Note: Torque spikes imply instability.)

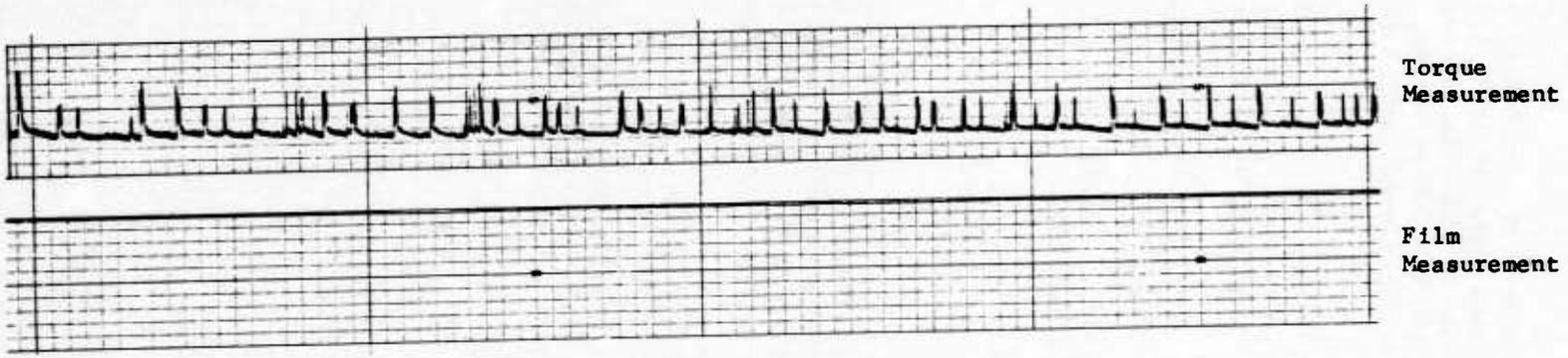

Chart Speed ~ 1 div = 5 sec.

FIGURE 13. BEARING TORQUE AND FILM MEASUREMENTS WITH "INDICATED ADEQUATE" LUBRICANTS

However, there is still some evidence of instability at full film lubrication. This is consistent with the results shown in Table III. There is also an experimental relation between loss of EHD film and torque fluctuation. It is not clear, however, whether the loss of film comes first or the instability. Stability has also been observed to be speed dependent occurring most often above 40 rpm.

The data from the laboratory experiment conducted thus far are in general agreement with the stability discussion of the preceding section and with Equation 3. Specified points of comparison are as follows.

(1) Stability is improved with lubrication and with lubricant quantity (i.e., h in Equation 3).

(2) Stability is directly affected by film thickness fluctuation or vise versa.

(3) Even with adequate lubrication, some instabilities still occur which is consistent with the calculation of Table III.

There are still some areas that merit further analysis such as the exact cause relationship between film thickness and torque fluctuation and the reason for the critical speed for instability. These, as well as other factors, will be explored in much more detail both experimentally as well as analytically in the second half of the research program.

Effect of Bearing Design Factors on Stability

Several experiments are being planned to evaluate the role of bearing design factors on cage instability. These experiments which have just been initiated will include evaluation of the following design factors.

The design factors being considered for experimental evaluations will be

(1) Contact Angle. Here it is planned that one contact angle (in addition to the 26 degree angle) will be evaluated. This angle will be significantly different than 26 degrees, although the exact angle is dependent on ball procurement by COMSAT.

(2) Effect of Cage Loading. Experiments will be conducted for various orientations of the g-vector relative to the spin axis.

(3) Cage Pocket Configuration. Experiments will be conducted for a ball-guided cage with at least two cone angles. In addition, two cage pocket-materials (phenolic and metal) will be used to evaluate the effect of cage stability of the pocket spring rate.

(4) Effect of Cage Control Surfaces. Experiments will be conducted with a race-guided cage as well as a ball-guided cage.

All of the experiments will be conducted at a speed of 100 rpm and a load of 60 lb at ambient temperature. The lubricant for these tests will be "Vackote". The experimental sequence will involve first determining if, for a given set of conditions, an instability can be induced. Experiments will then be conducted for cage loading conditions (see 2 above) near this instability point to establish the significance of the instability.

The above bearing test program is quite general in scope and is designed to be a reasonable adjunct to the analytical studies. However, since the experiments depend on the conditions promoting cage instability, it is very difficult to be much more specific in planning the experiments.

LIST OF REFERENCES

(1) Walters, C. T., "The Dynamics of Ball Bearings", J. Lub. Tech., Trans. ASME, Vol. 93, Series F, No. 1, January, 1971, pp. 1-10.

(2) Kannel, J. W., Dechow, J. P., and Walters, C. T., "Analysis of Separator Dynamics in a Low-Speed Despun Antenna Bearing", Proc. Int. Ball Bearing Symp., Charles Stark Draper Labs., June, 1973.

(3) Jones, A. B., "A General Theory for Elastically Constrained Ball and Roller Bearings Under Arbitrary Load and Speed Condition", Trans. ASME, J. Basic Eng., Vol. 82, Ser D, No. 2, June, 1960, pp 309-320.

(4) Bell, J. C., and Kannel, J. W., "Interpretations of the Thickness of Lubricant Films in Rolling Contact" 2. Influence of Possible Rheological Factors", Journal of Lubrication Technology, 93, Series F, Number 4, October, 1971.

(5) Bell, J. W., Kannel, J. W., and Allen, C. M., "The Rheological Behavior of the Lubrication in the Contact Zone of a Rolling Contact System", Journal of Basic Engineering, Trans. ASME, Series D 86, Vol. 83, No. 3, September, 1964, pp. 423-425.

(6) Benzing, R. J., Private Communication on Vackote 36233.

(7) Walters, C. T., Geer, T. E., Kannel, J. W., Sorenson, J. E., Brill, W. A., Lestingi, J., and Jones, A. B., "An Investigation of the Behavior of High Speed Angular Contact Ball Bearings Under Dynamic Load", Final Report to NASA-Marshall Space Flight Center, November 2, 1967, Contract NAS 8-20309.

(8) Seeley, F. B., and Smith, J. O., Advanced Mechanics of Materials, John Wiley & Sons, Inc., New York, Second Edition, p. 364, March, 1959.

NOMENCLATURE FOR APPENDICES

a - Half length of ball race contact area.

b - Half width of ball race contact area.

c - Subscript refer to contact at cage cone (Appendix F).

C_s - Race cage spring constant.

C_{s_1} - Ball cage interface spring constant (Equation B-10).

C_μ^1 - Ball race viscosity damping constant (Equation B-4).

CM - Center of mass.

D_p - Damping constant for ball race interface (Equation E-1).

d - Ball diameter.

e - Constant of restitution of ball cage impact. (Equation E-6)

f - Friction coefficient.

f_i, f_o - Race curvature.

F - Refers to force.

F_T - Ball-race tractive force.

F_c - Centrifugal force.

h - EHD film thickness.

i - Subscript for inner race (or input condition).

i_c - (Equation D-1).

K, K_i, K_o - Ball-race spring constants.

M_c - Cage mass.

M_e - Effective cage mass ($1/2\ M_c$)

m - Inner to outer race misalignment.

n - Refers to nth ball.

N_B - Number of balls in bearing.

o - Subscript for outer race (or output condition).

P_s, P_i, P_o - Ball loading.

P_h - Maximum Hertz pressure.

r_B - Ball radius.

R_p - Radius of Pitch.

s - Any normal position vector or

s - Subscript refers to static contact.

t - Time.

u - Velocity in y direction.

v - Velocity in y direction.

NOMENCLATURE FOR APPENDICES (Continued)

v - Velocity in y direction.

x - Coordinate variable.

y - Coordinate variable.

$\alpha_B(n)$ = Ball location angle for ball n.

$\alpha_c(n)$ - Cage location angle at ball n.

β - Cage center of mass rotational angle.

γ - Pressure coefficient of viscosity.

δ, δ_o, δ_1 - Deflection of an interface.

Δ, Δ_o, Δ_i - Ball race interface total deflection

ε - Radial clearance between ball and pocket.

ϕ - Cage cone angle (Figure F-1).

θ_c, θ_s, θ_o, θ_i - Bearing contact angle (Appendix A).

ρ - Radial location of cage center of mass (Figure 3).

ρ_m - Maximum value of ρ.

ν - Poisson's ratio.

APPENDIX A

BEARING STRESS COMPUTATIONS

APPENDIX A

BEARING STRESS COMPUTATIONS

The purpose of this Appendix is to outline the approach for determining the ball-race contact stresses and dimensions. This approach involves first computing the stresses for a static (nonrotating) bearing and then computing the effect of centrifugal forces on contact angles. The equations have been abstracted from the works of A. B. Jones.[3,7]

Static Analyses

Under static contact, the bearing can be subject to both axial (including misalignment) and radial loads. For the purpose of the analysis this implies that the deflection of each ball-race interface in the bearing must produce forces which sum to the applied radial and axial loads.

Deflections

Referring to Figure A-1, the vertical, A_2, and horizontal, A_1, separations of the race curvature centers can be expressed as

$$A_1(n) = Bd \sin\theta_d + \delta_0 + m R_p \cos\left(\frac{2\pi(n-1)}{N_B}\right) , \qquad (A-1)$$

and

$$A_2(n) = Bd \cos\theta_d + \delta_1 \cos\left(\frac{2\pi(n-1)}{N_B}\right) . \qquad (A-2)$$

Here, d is the ball diameter, θ_d is the design contact angle, m is the misalignment, R_p is the pitch radius, n refers to the nth ball, N_B is the total number of balls, δ_0 and δ_1 are the axial and radial deflections to be determined and

$$B = f_o + f_i - 1, \qquad (A-3)$$

where $f_{o,i}$ are the outer and inner race curvatures. (Bd is the distance between curvature centers.)

The total deflection of the ball race interface (for each ball) can be written

$$\Delta(n) = \sqrt{A_1^2 + A_2^2} - Bd , \qquad (A-4)$$

and the contact angle after deflection becomes

$$\theta_s = \tan^{-1}\frac{A_1}{A_2} . \qquad (A-5)$$

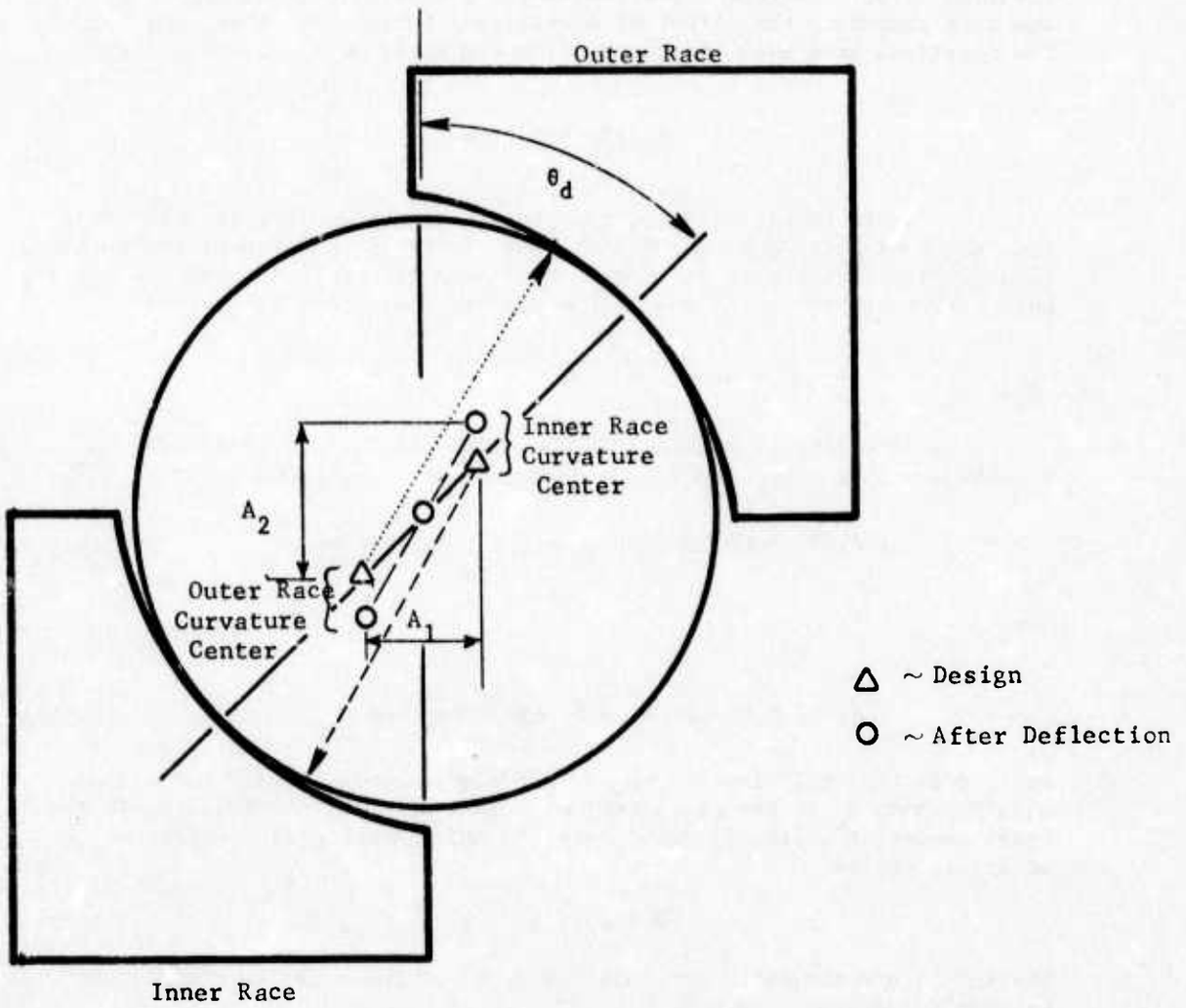

FIGURE A-1. NOMENCLATURE FOR STATIC ANALYSES

Force Equilibrium

The force at each ball contact can be written in terms of deflection by

$$P_s(n) = K(n)\,\Delta^{\frac{3}{2}} ,$$

where K is the interfacial spring constants given by

$$\frac{1}{K} = \left[\frac{1}{K_o^{\frac{2}{3}}} + \frac{1}{K_i^{\frac{2}{3}}} \right]^{\frac{3}{2}} . \qquad \text{(A-7)}$$

Here $K_{o,i}$ are the ball race spring constants for the outer and inner race contact. These constants are defined, for example, in Equations B-6, B-7, and B-8.

Ignoring gyroscopic effects, the force summation requires that

$$F_A = \sum_{n=1}^{N_B} P_s \sin \theta_s , \qquad \text{(A-8)}$$

and

$$F_R = \sum_{n=1}^{N_B} P_s \cos \theta_s \sin \left[\frac{2\pi(n-1)}{N_B} \right] , \qquad \text{(A-9)}$$

where F_A and F_R are the total axial and radial force components. Equations A-1 to A-9 have been solved using a double nesting procedure. This procedure essentially involves guessing values of δ_0 and δ_1 and computing A_1 and A_2 (Equations A-1 and A-2) and, in turn Δ, θ_d, P, and finally F_A and F_R. Logical guesses of δ_0 and δ_1 are made until F_A and F_R are equal to the applied loadings.

Effect of Centrifugal Force

The primary assumption used here is that centrifugal force alters the inner and outer race contact angles (and associated forces) but does not affect the ball-to-ball load sharing.

Deflection Equations

The deflection of the inner and outer race contacts as well as the contact angles will, of course, now be somewhat different. Referring to Figure A-2 it can be seen that

$$\Delta_o(n) = \sqrt{X_1^2 + X_2^2} - (f_o - 0.5)\,d , \qquad \text{(A-10)}$$

and

$$\Delta_i(n) = \sqrt{(A_1 - X_1)^2 + (A_2 - X_2^2} - (f_i - 0.5)\,d . \qquad \text{(A-11)}$$

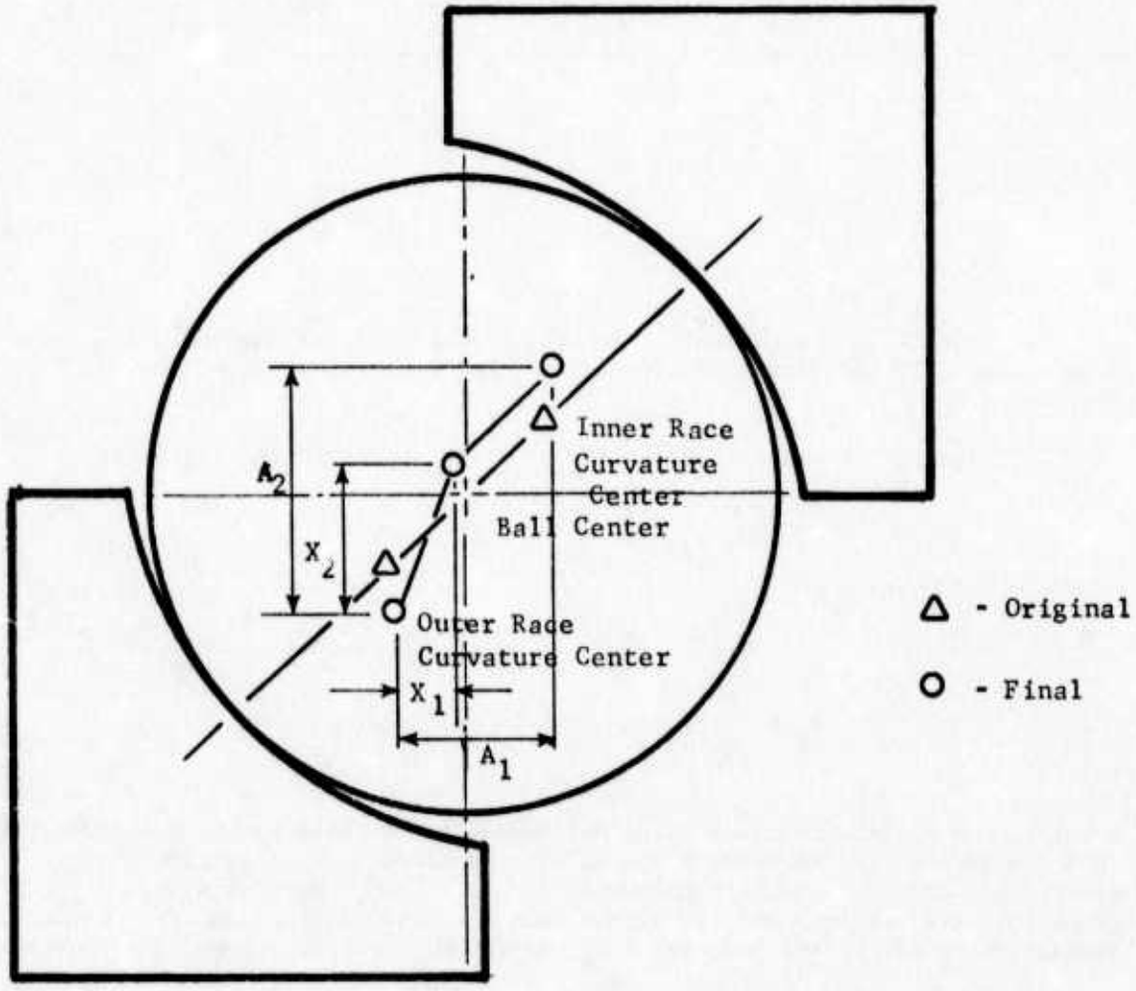

FIGURE A-2. NOMENCLATURE FOR CENTRIFUGAL FORCE EFFECTS

Likewise

$$P_i = K_i \Delta_i^{\frac{3}{2}} \quad \text{and} \quad P_0 = K_0 \Delta^{\frac{3}{2}} \quad . \tag{A-12}$$

Also

$$\theta_o = \tan^{-1} \frac{X_1}{X_2} \quad , \tag{A-13}$$

and

$$\theta_i = \tan^{-1} \left[\frac{A_1 - X_1}{A_2 - X_2} \right] \quad . \tag{A-14}$$

Force Equilibrium

The force equilibrium between inner and outer race, ignoring gyroscopic force effects, can be written

$$P_0 \sin \theta_o = P_i \sin \theta_i \quad , \tag{A-15}$$

and

$$P_0 \cos \theta_o = P_i \cos \theta_i + F_c \quad . \tag{A-16}$$

The assumption that centrifugal effects do not affect ball-ball load sharing implies that

$$P_i \sin \theta_i = P_s \sin \theta_s \quad . \tag{A-17}$$

Solution

By combining Equations A-15 and A-16 there results

$$\frac{1}{\tan \theta_o} = \frac{1}{\tan \theta_i} \frac{F_c}{P_s \sin \theta_s} \qquad \text{(A-18)}$$

By guessing (by a nesting process), a value of θ_i, θ_o can be computed. With these values of θ_i and θ_o, X_1 and X_2 can be computed from Equations A-13 and A-14 for the known (from the static analysis) value of A_1 and A_2. Equations A-10 to A-12 can now be used to determine a value of P_i. The correct guess of θ_i will produce a value of P_i which is consistent with Equation A-17.

APPENDIX B

SPRING AND DAMPING CONSTANTS

APPENDIX B

SPRING AND DAMPING CONSTANTS

Ball-Race Force-Traction Relationship

If it is assumed that the ball and race in a bearing are separated by a thin layer of lubricant of thickness, h, then the ball-race tractive force can be written

$$F_T = \iint_A \tau \, dA \quad , \tag{B-1}$$

where τ is the shear stress and A is the contact area. It can be shown[5] that

$$\tau = \mu \frac{\partial u}{\partial y} = \mu_i e^{\gamma p} \frac{\Delta U}{h} \quad . \tag{B-2}$$

Here ΔU is the slip at the ball-race interface, μ_i is the base viscosity, p is the contact pressure, and γ is a constant pressure viscosity coefficient. It is assumed that the contact pressure distribution is Hertzian, i.e.,

$$p = p_h \sqrt{1 - \frac{x^2}{a^2} - \frac{z^2}{b^2}} \quad , \tag{B-3}$$

where p_h is the maximum contact pressure and a and b are the major and minor axis of the contact ellipse.

By combining Equations B-1 through B-3 there results[5]

$$F_T = C_\mu \Delta U \quad ,$$

$$C_\mu = \frac{2\pi ab\mu_i}{h\gamma^2 p_h^2} \left[e^{\gamma p_h} (\gamma p_h - 1) + 1 \right] \tag{B-4}$$

For a given ball race, contact situation the ball race traction is then dependent only on a constant, C_μ, and the slip condition.

Normal Force Between Ball and Cage Pocket

A reasonable assumption for the ball-cage contact is that it represents an elastic-spring mass system. The force deflection relationship for two elastic bodies in contact can be written (from Sealy and Smith[8], page 364).

$$P = \left[\frac{\pi C_b}{C_\delta (A+B)}\right]^{\frac{3}{2}} \frac{\delta^{\frac{3}{2}}}{\Delta} = C_s \delta^{\frac{3}{2}} \quad , \tag{B-5}$$

where P is load, C_b and C_δ are constants, and

$$A = \tfrac{1}{2}\left[\frac{1}{r_B} - \frac{1}{r_p}\right] \quad , \quad B = \frac{1}{2r_B} \quad , \tag{B-6}$$

$$\Delta = \frac{1}{A+B}\left(\frac{1-\nu_p^2}{E_p} + \frac{1-\nu_B^2}{E_B}\right) \quad . \tag{B-7}$$

Here δ is the deflection, r is radius, ν is Poisson's ratio, E is Young's modulus, and the subscripts p and B refer to pocket and ball, respectively.

Similar equations can be written for the cage-race contact. Here r_B would be the race radius and r_p would be the cage radius. The parameter B would also be somewhat modified to accommodate the different contact geometry condition.

The constant C_b and C_δ can be approximated by

$$C_b \approx 0.635 \left(\frac{B}{A}\right)^{-0.1722} \text{ and } C_\delta \approx 3.214 \left(\frac{B}{A}\right)^{-0.471} \quad . \tag{B-8}$$

Equation B-5 involves the use of a single constant, C_s, and the deflection to determine ball-cage forces.

A very useful simplification would occur if Equation B-5 could be approximated by a linear, rather than a 3/2 power spring in the form

$$P \approx C_{s_1} \delta \quad . \tag{B-9}$$

If a typical value of P is say 0.2 lb, then Equations B-5 and B-9 would produce the same load for this condition provided that

$$C_{s_1} \approx 0.6\, C_s^{\frac{2}{3}} \quad . \tag{B-10}$$

Similarly, C_{s_2} can be computed for a cage-race contact.

APPENDIX C

CENTER OF MASS LOCATION (INCLUDING RACE GUIDED CAGE INFLUENCE)

APPENDIX C

CENTER OF MASS LOCATION (INCLUDING RACE GUIDED CAGE INFLUENCE)

Center-of-Mass Location

Referring to Figure 3, the equation of motion for radial displacement of the cage CM can be written (in the absence of ball contact)

$$\ddot{\rho} + \frac{F_s}{M_c} - F_c = 0 \quad , \tag{C-1}$$

where M_c is the mass of the cage, ρ is the radial displacement and

$$F_s = \begin{cases} C_s\,(\rho - \rho_m) & \text{if } \rho > \rho_m \\ 0 & \text{if } \rho < \rho_m \end{cases} \quad , \tag{C-2}$$

and, it is helpful to define F_c, such that

$$F_c = \begin{cases} \dot{\beta}^2 \rho & \text{if } \rho < \rho_m \\ \dot{\beta}^2 \rho_m & \text{if } \rho > \rho_m \end{cases} \quad .$$

Here ρ_m is the maximum free movement of the cage and C_s is an assumed linear spring constant. Thus, F_s characterizes the cage-race radial contact force and F_c characterizes the centrifugal force acting on the cage CM.

Solution for $\rho < \rho_m$

For this condition the solution to Equation C-1 can be written

$$\rho = \begin{cases} C_1 \sinh (A + \dot{\beta} t) & \text{if } C_1 \text{ real} \\ iC_1 \cosh (A + \dot{\beta} t) & \text{if } C_1 \text{ imaginery} \end{cases} \quad . \tag{C-3}$$

By designating ρ_i and $\dot{\rho}_i$ as the initial radial location and velocity of the CM, respectively, then

$$C_1 = \sqrt{\frac{\dot{\rho}_i^2}{\dot{\beta}^2} - \rho_i^2} \quad ,$$

and

$$A = \begin{cases} \sinh^{-1}\left(\frac{\rho_i}{C_1}\right) & \text{if } C_1 \text{ real} \\ \cosh^{-1}\left(\frac{\rho_i}{iC_1}\right) & \text{if } C_1 \text{ imaginary} \end{cases} \quad . \qquad \text{(C-4)}$$

Equation C-3 can be inverted to determine the time when, for example, $\rho = \rho_m$ as well as being used to compute ρ for a given time step.

Solution for $\rho > \rho_m$

The solution of this equation can be written

$$\rho = C_1' \sin(A' + Bt) + C_2 \quad , \qquad \text{(C-5)}$$

where

$$B = \sqrt{\frac{C_s}{M_c}} \quad \text{and} \quad C_2 = \left(1 + \dot{\beta}^2 \frac{M_c}{C_s}\right)\rho_m \quad . \qquad \text{(C-6)}$$

Using the same initial conditions as above, it can be shown that

$$A' = \tan^{-1}\left[\frac{B(\rho_i - C_2)}{\dot{\rho}_i}\right] \quad \text{and} \qquad \text{(C-7)}$$

$$C_1' = \frac{\dot{\rho}_i}{B\cos(A')} \quad . \qquad \text{(C-8)}$$

The cage and race will come out of contact where $\rho = \rho_m$ in Equation C-5 when

$$t = \frac{\pi}{B} - \frac{A'}{B} - \frac{\sin^{-1}}{B}\left[-\frac{\dot{\beta}^2 M_c}{C_{s_2}}\frac{\rho_m}{C_1}\right] \qquad \text{(C-9)}$$

APPENDIX D

MOMENTUM TRANSFER TO CAGE CYLINDER AT IMPACT

APPENDIX D

MOMENTUM TRANSFER TO CAGE CYLINDER AT IMPACT

Momentum Transfer at Ball-Cage Impact

For each time step, the computer program determines value of the following parameters and their time derivative (see Figure D-1)

$\alpha_c(n)$ = The angular position of the cage at any ball location-n

$\alpha_B(n)$ = The angular position of the ball-n

β = The angular position of the cage-CM

ρ = The radial position of the cage-CM.

Impact Criterion

Impact will occur between ball and cage for any ball-n when CHK is less than zero, where

$$CHK = \begin{cases} [\alpha_c + \rho/R_p \sin(\beta - \alpha_c)] - \alpha_B + \epsilon & \text{front } (i_c = -1) \\ \alpha_B - [\alpha_c + \rho/R_p \sin(\beta - \alpha_c)] + \epsilon & \text{back } (i_c = 1). \end{cases} \quad \text{(D-1)}$$

Where R_p is the pitch radius and ϵ is the radial clearance between ball and pocket. At front contact (see Figure D-1) i_c is set equal to (-1) and at back contact i_c is set equal to +1.

Impact Velocity

At impact, the components of velocity of the CM of the cage can be written (in terms of known parameters) as follows

$$\dot{x}_i' = \dot{\rho}_i \sin\beta + \rho\dot{\beta}_i \cos\beta$$

$$\dot{y}_i' = \dot{\rho}_i \cos\beta - \rho\dot{\beta}_i \sin\beta \quad \text{(D-2)}$$

where the i subscript refers to impact condition.

The approach velocity of the cage to ball, u, can be written

$$u_i = R_p(\dot{\alpha}_c - \dot{\alpha}_B) + \dot{x}_i' \cos\alpha_c - \dot{y}_i' \sin\alpha_c, \text{ and}$$

$$v_i = \dot{x}_i' \sin\alpha_c + \dot{y}_i' \cos\alpha_c \quad \text{(D-3)}$$

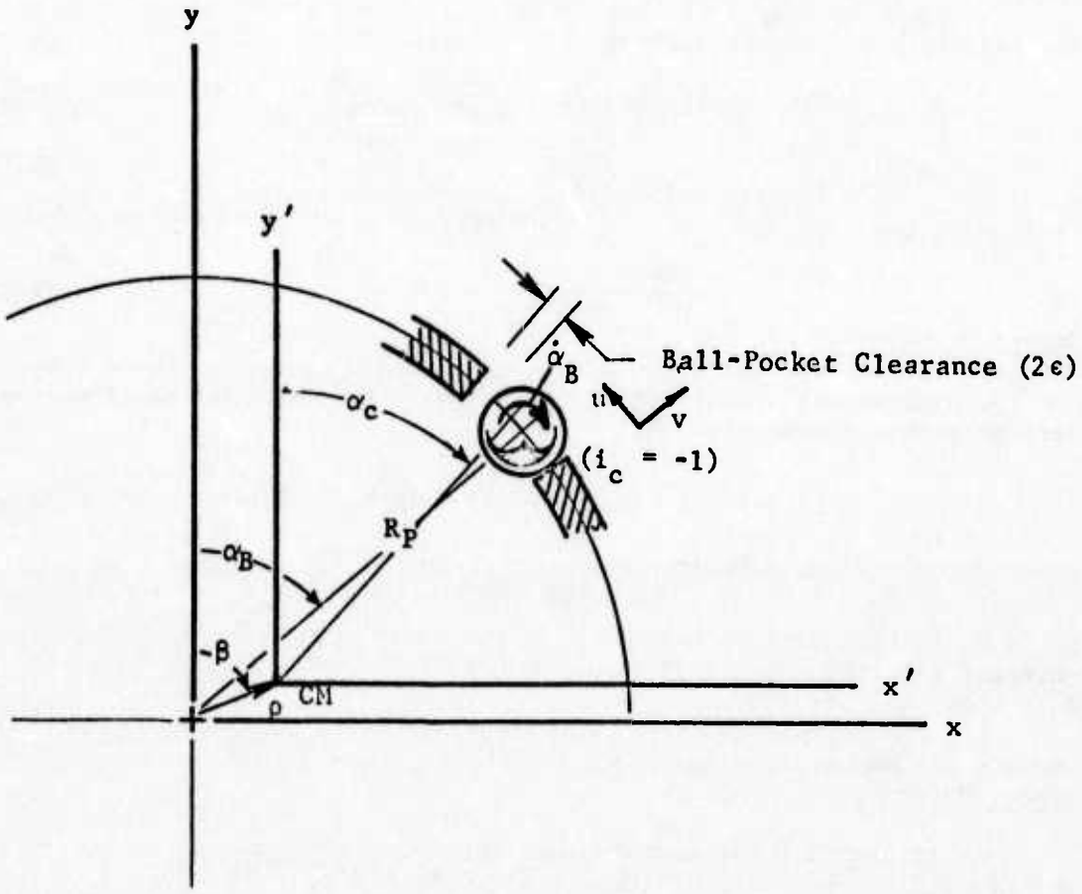

FIGURE D-1. COORDINATE SYSTEM FOR CAGE-BALL LOCATIONS
(Illustration of Front Contact)

Momentum Transfer

During impact, the velocity component u and v are altered. The alteration of u is as described in Appendix E. Following impact,

$$u_o = -u_i\, e \quad , \tag{D-4}$$

where e is a constant of restitution. The o and i refer to output velocity and input velocity, respectively. The change in the velcotity v can be derived from momentum considerations as follow

$$Mdv = F_y dt \quad , \text{ since} \tag{D-5}$$

$$Mdu = F_x dt \quad , \text{ and since} \tag{D-6}$$

$$F_y = fF_x \quad , \tag{D-7}$$

there results

$$v_o - v_i = f(u_o - u_i) \quad , \tag{D-8}$$

where f is the friction coefficient and F_x and F_y refer to force components at the cage impact. In reality, however v_o cannot exceed the linear velocity of the ball surface v_B so that

$$v_o = \begin{cases} [v_i + f(u_o - u_i)i_c] & \text{if } v_o < v_B \\ v_B\, i_c & \text{otherwise.} \end{cases} \quad . \tag{D-9}$$

Dispart Velocity

The alteration of the velocity components u and v will, of course, modify the center of mass velocity components or*

$$\dot{x}_o' - \dot{x}_i' = \left(\frac{u_o - u_i}{2}\right) \cos\alpha_c + (v_o - v_i) \sin\alpha_c, \text{ and}$$

$$\dot{y}_o' - \dot{y}_i' = -\left(\frac{u_o - u_i}{2}\right) \sin\alpha_c + (v_o - v_i) \cos\alpha_c \quad . \tag{D-10}$$

Finally, by inverting Equation D-2, there results

$$\dot{\rho} = \dot{x}_o' \sin\beta + \dot{y}_o' \cos\beta, \text{ and}$$

$$\rho\dot{\beta}_o = \dot{x}_o' \cos\beta - \dot{y}_o' \sin\beta \quad . \tag{D-11}$$

* It is assumed here that $I = M_c R_p^2$, where I is the cage mass moment of inertia and M_c is the cage mass.

The dispart angular velocity of the cage can be written

$$(\dot{\alpha}_o - \dot{\alpha}_i) = \left(\frac{u_o - u_i}{2R_p} \right) \qquad \text{(D-12)}$$

APPENDIX E

IMPACT OF BALL AND CAGE

APPENDIX E

IMPACT OF BALL AND CAGE

Under impact conditions, a force will be exerted on the cage which, if sufficiently large, can affect the cage motion adversely and, possibly, can perpetrate an instability. To examine the condition under which an instability might occur, consider the force diagram of Figure E-1b. Here C_μ and C_s are the constants described by Equations B-4 and B-9, M_e is the effective mass of the cage, δ is the deflection of the cage at the ball-cage interface, and $\dot{s}$ is the cage velocity. For equilibrium of the forces ignoring ball mass in comparison to ball race friction, it can be shown that

$$\begin{aligned} C_\mu(\dot{\delta}-\dot{s}) &= -C_{s_1}\delta \\ -C_s\delta &= M_e\ddot{s} \end{aligned} \qquad \text{(E-1)}$$

where M_e is the effective mass of the cage. (This can be shown to equal $1/2\ M_c$.) By performing an integration, the above two equations can be combined to yield (the constant of integration has been ignored for convenience).

$$\ddot{s} + \frac{C_{s_1}}{C_\mu}\dot{s} + \frac{C_{s_1}}{M_e}s = 0 \quad . \qquad \text{(E-2)}$$

The initial conditions on s are taken to be given by

$$s(0) = 0, \quad \dot{s}(0) = \dot{s}_o \quad , \qquad \text{(E-3)}$$

where $\dot{s}_o$ is the cage velocity at the onset of the impact between the cage and the ball. The form of the solution for Equation E-2 depends on the magnitude of the parameter $4C_\mu^2/M_eC_{s_1}$. If

$$D_p \equiv \frac{4C_\mu^2}{M_eC_{s_1}} > 1 \quad , \qquad \text{(E-4)}$$

then, the solution of Equation E-2 satisfying the initial conditions is

$$s = \frac{\dot{s}_o}{C_1}e^{-C_2t}\sin C_1t \, , \qquad \text{(E-5)}$$

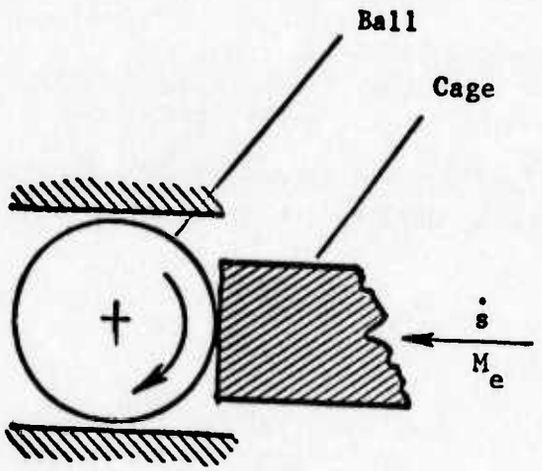

(a) Ball-Cage Impact

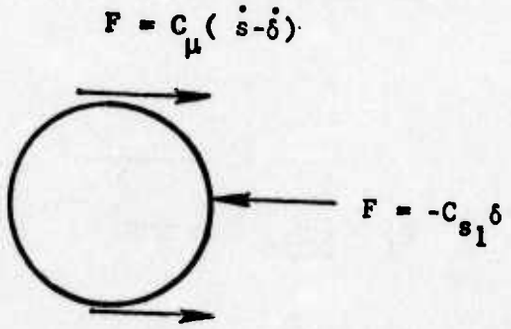

(b) Force Diagram

FIGURE E-1. FORCE DIAGRAM FOR BALL-CAGE IMPACT

where

$$C_1 = \frac{C_{s_1}}{2C_\mu}\sqrt{\frac{4C_\mu^2}{M_e C_{s_1}} - 1} \quad ,$$

and

$$C_2 = \frac{C_{s_1}}{2C_\mu} \quad .$$

The rebound velocity $\dot{s}_r$ will be the value of $\dot{s}$ when $C_1 t = \pi$ or

$$\dot{s}_r = \dot{s}_o \left(\exp\left(\frac{-C_2\pi}{C_1}\right)\right) \equiv e\ \dot{s}_o \qquad \text{(E-6)}$$

On the other hand if

$$D_p = \frac{4C_\mu^2}{M_e C_{s_1}} < 1 \quad , \qquad \text{E-7)}$$

then the solution is

$$s = \frac{\dot{s}_o}{C_1'} e^{-C_2 t} \sinh C_1' t \quad , \qquad \text{(E-8)}$$

where

$$C_1' = \frac{C_{s_1}}{2C_\mu}\sqrt{1 - \frac{4C_\mu^2}{M_e C_{s_1}}} \quad , \qquad \text{(E-9)}$$

It is noted that the solution given by Equation E-5 denotes an oscillatory motion of the cage. This is taken to imply that the cage motion is unstable. The solution given by Equation E-8 indicates that the ball-cage contact will absorb the effects of the cage-ball impact, and, hence, the motion of the cage is not oscillatory. Under this latter condition, the cage should be stable.

APPENDIX F

MOMENTUM TRANSFER TO CAGE-CONE AT IMPACT

APPENDIX F

MOMENTUM TRANSFER TO CAGE-CONE AT IMPACT

Ball-Pocket Impact for Ball-Guided Cage

The geometry being analyzed is illustrated in Figure F-1 and involves a cone-cylinder cage pocket. Ball contact can occur either at the cylindrical surface region or at the conical surface region. The impact conditions will be assumed to be similar for both cases though somewhat more complex transformations are required for the cone contact.

Description of Cone Region

At least two parameters, in addition to the pocket radius, are needed to define the location of the cone contact relative to the ball.

(1) The cone angle, ϕ.

(2) The perpendicular distance between the center of the ball and the base of the cone surface, y_s.

The second of the above locating coordinates is related to the cage design and the location of the cage center of mass relative to the ball. That is

$$y_s = y_d - y_{cm} \quad , \tag{F-1}$$

where y_d is the distance between the center of the ball and the base of the cone for a perfectly centered cage and y_{cm} is the radial location of the cage center of mass. It can be shown that

$$y_{cm} = \rho \cos (\beta - \alpha_c) \quad , \tag{F-2}$$

where ρ, β, and α_c are the locating coordinates for a point on the cage (Figure 3). For the case where $y_{cm} = 0$, the ball will make simultaneous contact with the cone and the cylinder if

$$y_d = r_B \frac{(1 - \cos\phi)}{\sin \phi} \quad , \tag{F-3}$$

where r_B is the ball radius. The value of y_d given by Equation F-3 should represent a reasonable design for the cage to be ball guided.

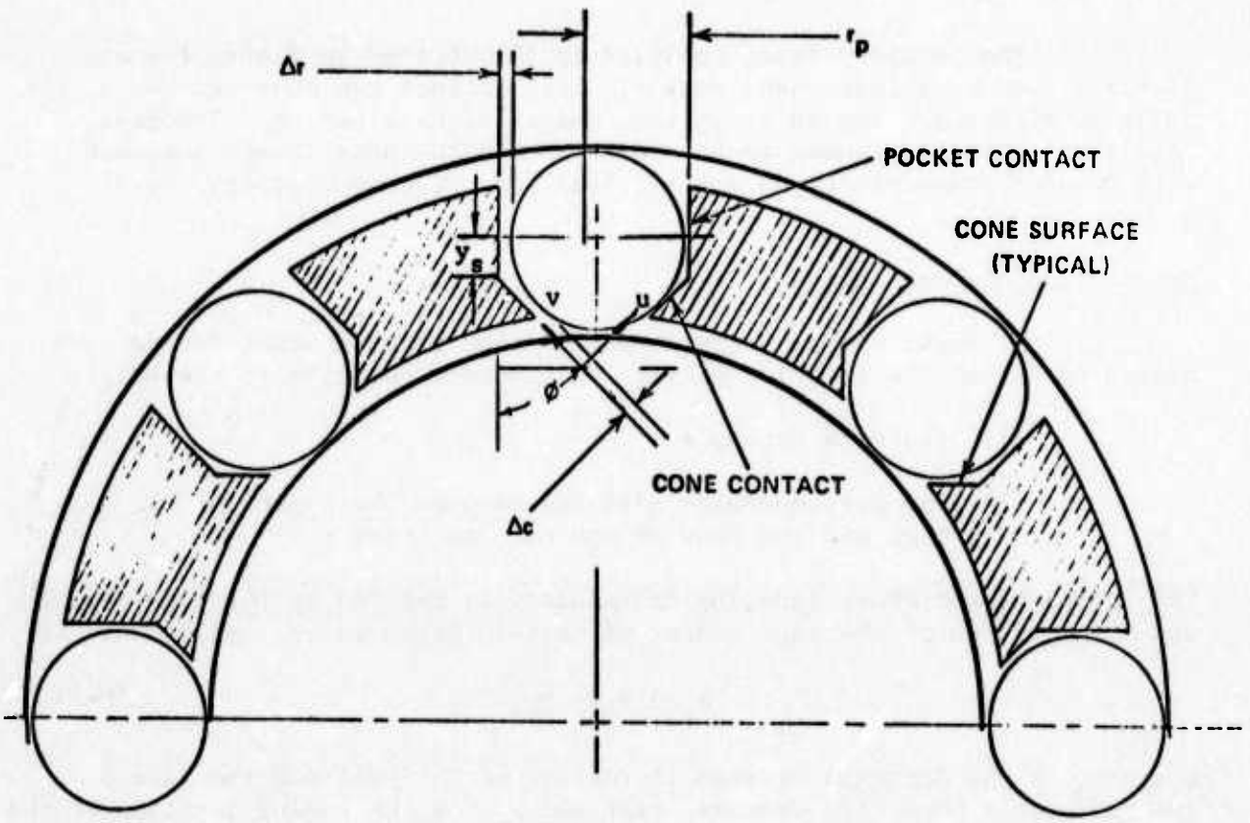

FIGURE F-1. GEOMETRY OF BEARING ANALYZED

Criterion for Contact

The clearance between ball and cylinder (Figure F-1) can be expressed

$$\Delta r = r_p - r_B - \delta_T \quad , \tag{F-4}$$

where δ_T represents the tangential movement of the cage relative to the ball. The corresponding clearance between ball and cone can be written

$$\Delta c = r_P - \frac{r_B}{\cos\phi} + y_s \tan\phi - \delta_T \quad . \tag{F-5}$$

The relationship between cone and cylinder clearance can be expressed

$$\Delta c = \Delta r - r_B \left(\frac{1 - \cos\phi}{\cos\phi} \right) + y_s \tan\phi \quad . \tag{F-6}$$

It can be seen that for the case where $\phi = 0$ or for $y_s = y_d$ (using Equation F-3), $\Delta c = \Delta r$. In the computer routine, it is necessary to check the level of Δc versus Δr at the contact conditions to establish whether contact occurs at the cylinder or at the cone, or at both surfaces simultaneously.

Impact and Rebound Velocity Components

The impact velocity components u and v of Figure F-1 are analogous to the components for ball-cylinder contact but only at a skewed angle. The transformation of the ball-cylinder velocity equation into cone contact velocities can be written

$$u_c = u_i \cos\phi + v_i \sin\phi \quad , \text{ and} \tag{F-7}$$

$$v_c = -u_i \sin\phi + v_i \cos\phi \quad . \tag{F-8}$$

Here, the subscript c refers to cone contact and u_i and v_i are the impact tangential and radial velocity components, respectively, discussed in Appendix D (Equation D-4 and D-9). Following impact, the rebound radial and tangential velocity components can be expressed

$$u_o = u_{c_o} \cos\phi - v_{c_o} \sin\phi \quad , \text{ and} \tag{F-9}$$

$$v_o = u_{c_o} \sin\phi + v_{c_o} \cos\phi \quad . \tag{F-10}$$

Here, the subscript, c_o refers to the rebound condition at the ball cone interface.

Equation F-7 through F-10 are incorporated into the transformation subroutine to account for any type of cone contact. If, for example, a zero angle is used, u_c and v_c revert to simply u_i and v_i and, concomitantly u_o and v_o are the same as u_{c_o} and v_{c_o}.

☆ U. S. GOVERNMENT PRINTING OFFICE: 1975 — 657-630/137